Zeitschrift: Helvetica Physica Acta
Band: 45 (1972)
Heft: 7

Artikel: Experimental angular correlation functions of molecules in liquids and in crystals
Autor: Keller, Bruno / Kneubühl, Fritz
DOI: https://doi.org/10.5169/seals-114432

Helvetica Physica Acta
Vol. 45, 1972.

Birkhäuser Verlag Basel

Experimental Angular Correlation Functions of Molecules in Liquids and in Crystals

by **Bruno Keller** and **Fritz Kneubühl**

Solid State Physics Laboratory, ETH, Zürich

(21. VIII. 72)

Abstract. In this paper we describe the experimental investigation of molecular reorientation processes with the aid of angular correlation functions. After a brief summary of the theory the experimental limitations are outlined. Subsequently this method is applied to HCl and DCl dissolved in liquid tetrachlorides and to OD^--ions in alkalihalides. Models for the short time behaviour of these dipoles are presented. The applicability of the angular correlation functions is extended to polyatomic molecules by group theoretical considerations. Experimental examples are presented.

Zusammenfassung. Die vorliegende Arbeit befasst sich mit der experimentellen Untersuchung von molekularen Reorientierungsprozessen mit Hilfe von zeitabhängigen Richtungskorrelationsfunktionen. Nach einer kurzen Zusammenfassung der Theorie werden die experimentellen Grenzen der Methode diskutiert. Als Anwendung werden die Systeme von HCl und DCl in flüssigen Tetrachloriden und von OD^--Ionen in Alkalihalogeniden untersucht. Das Kurzzeitverhalten dieser Dipole wird an Hand von Modellen gedeutet. Mit Hilfe gruppentheoretischer Methoden wird der Anwendungsbereich der Korrelationsfunktionen auf mehr als zwei-atomige Moleküle ausgedehnt und die Resultate an einigen experimentellen Beispielen erläutert.

1. Introduction

Since the days of P. Debye [1] considerable effort was taken to obtain information on the microscopic mechanism of reorientation of molecules in liquids and solids. Most of the work dealt with the measurement of spectroscopic line widths and relaxation times derived therefrom, yielding one single parameter to characterize the complicated processes [2]. Moreover, different spectroscopic techniques led to contradicting results.

Fortunately in recent years linear response theory [3, 4] provided the tool to interpret the line shapes of rotating molecules in terms of time-dependent correlation functions [5, 6]. These correlation functions are obtained as Fourier transforms of the corresponding line profiles. They give a detailed description of the average molecular motion over a restricted time range. In addition the introduction of correlation functions allows us to profit from the theory of stochastic processes [7, 8, 9, 10] and to test many of the deductions of the earlier theories on a more general basis.

The purpose of this study is to demonstrate the fruitfulness of the correlation function method as well as to discuss the inherent experimental limitations and difficulties. It is applied to the vibration-rotation spectra of diatomic and polyatomic molecules in liquids and diatomic impurities in alkalihalides.

A number of excellent theoretical reviews exists on the subject [2, 4, 11–14]. The principal results necessary for the comprehension of the experimental work are summarized in Section 2. Section 3 is dedicated to the evaluation of correlation and

memory functions from experimental infrared spectra. The next three sections deal with the application of the method to diatomic molecules dissolved in liquids, diatomic impurities in alkalihalides and simple polyatomic molecules in liquids respectively. Finally, the Appendix presents the angular correlation functions of polyatomic molecules required for the interpretation of vibrational Raman spectra.

2. Basic Concepts of Correlation Functions

2.1. *Linear response theory*

For an *outline of the basic ideas* [3, 11] of the linear response theory we consider a macroscopic sample consisting of a large number of molecules in thermal equilibrium described by a Hamiltonian H and a thermal distribution function f. Information on the expectation value $\langle A(t)\rangle$ of a microscopic variable A, e.g. the spatial component $(\vec{e}\cdot\vec{\mu})$ of the electric dipole moment $\vec{\mu}$, is provided by the response of the sample to a weak force F, e.g. the electric field $\vec{E}$, acting on this variable.

In *classical statistical mechanics* the equation of motion for the equilibrium distribution f is

$$\frac{\partial f}{\partial t} = [H,f] = 0. \tag{2.1}$$

The perturbation $\Delta H = A\,F$ gives rise to a change Δf of the distribution function

$$\frac{\partial \Delta f}{\partial t} = [H,\Delta f] + [\Delta H,f] + [\Delta H,\Delta f]. \tag{2.2}$$

If the ensemble is in stable equilibrium and if the force F fulfils the condition

$$|A\cdot F| \ll H \tag{2.3}$$

the second-order term $[\Delta H, \Delta f]$ can be neglected. Hence $\langle A(t)\rangle$ depends linearly on $F(t)$:

$$\langle \Delta A(t)\rangle = \int_{-\infty}^{t} \phi_A(t-t')\,F(t')\,dt' \tag{2.4}$$

with the *response function*:

$$\phi_A(t-t') = -\int_{\Gamma} [A,f]_{t'}\cdot A(t)\cdot d\Gamma, \tag{2.5}$$

where Γ represents the phase space.

In the canonical ensemble

$$f = e^{-H/kT}\Big/\int_{\Gamma} e^{-H/kT}\,d\Gamma \tag{2.6}$$

one finds

$$\begin{aligned}\phi_A(t-t') &= -\frac{1}{kT}\int f\frac{\partial A(t')}{\partial t'}\,A(t)\,d\Gamma \quad \text{equil.}\\ &= -\frac{1}{kT}\left\langle \frac{\partial A(t')}{\partial t'}\,A(t)\right\rangle \quad \text{equil.}\end{aligned} \tag{2.7}$$

For a constant force switched off at the time $t = 0$ the system relaxes according to

$$\langle A(t)\rangle = +F \int_t^\infty \phi_A(t')\, dt' = F\Phi_A(t) \tag{2.8}$$

with the *relaxation or correlation function*

$$\Phi_A(t) = \int_t^\infty \phi_A(t')\, dt' = -\frac{1}{kT}\{\langle A(0)\, A(t)\rangle - \langle A^2(0)\rangle\}. \tag{2.9}$$

For a periodic force

$$F(t) = F_0 \cdot \cos \omega t.$$

the *complex susceptibility* $\chi_A(\omega)$ defined by

$$\langle \Delta A(t)\rangle = \mathrm{Re}\,\chi_A(\omega)\, F_0\, e^{-i\omega t} \tag{2.10}$$

is related to the correlation function $\Phi_A(t)$

$$\chi_A(\omega) = \chi'_A(\omega) - i\chi''_A(\omega) = \Phi_A(0) - i\omega \int_0^\infty \Phi_A(t)\, e^{-i\omega t}\, dt. \tag{2.11}$$

The relation of $\Phi_A(t)$ to the quantum mechanical correlation function is discussed in Section 2.4.

2.2. *General properties of autocorrelation functions*

Many physical ensembles are stationary and ergodic. Wide sense *stationarity* is characterized by a time-independent average $\langle A(t)\rangle$ and by a correlation function $\langle A(t_1)\, A(t_2)\rangle$ which depends only on the time difference $t = t_2 - t_1$

$$\Phi(t) = \langle A(t_1)\, A(t_2)\rangle = \langle A(0)\, A(t)\rangle. \tag{2.12}$$

According to Onsager [15] the *microscopic reversibility* of physical processes requires

$$\Phi(-t) = \Phi(t). \tag{2.13}$$

Moreover any correlation function of a *stationary-random process* has to be non-negative definite [7, 9]:

$$\Phi(0) \geqq |\Phi(t)|. \tag{2.14}$$

The *first two derivatives of an autocorrelation function* $\Phi(t)$ of a real physical quantity should exist. Equation (2.13) yields

$$\frac{d}{dt}\Phi(t)\bigg|_{t=0} = 0 \tag{2.15}$$

and equation (2.14)

$$\frac{d^2}{dt^2}\Phi(t)\bigg|_{t=0} = -\langle \dot{A}(0)\, \dot{A}(t)\rangle_{t=0} < 0. \tag{2.16}$$

Ergodicity [8, 10] permits the replacement of the phase-space average by a time average over a trajectory

$$A(t) = \lim_{T \to \infty} T^{-1} \int_0^T A(t)\, dt. \tag{2.17}$$

Since the correlation function $\Phi(t)$ describes the fluctuations of $A(t) - \langle A(t) \rangle$ the relation

$$\lim_{T \to \infty} T^{-1} \int_0^T \Phi(t)\, dt = 0 \tag{2.18}$$

holds. Therefrom an upper limit for $\Phi(t)$ can be deduced [7]:

$$|\Phi(t)| < K(1 + t^{\gamma})^{-1} \tag{2.19}$$

with $0 < \gamma < 1$, and K as an arbitrary constant.

2.3. *Memory functions and Onsager separability*

Antecedent to linear response theory the usual procedure for dealing with rotational relaxation phenomena was based on the *Langevin equation* [11], e.g. for a linear molecule

$$\frac{d}{dt} \vec{J}(t) = -\beta \vec{J}(t) + \vec{N}(t) \tag{2.20}$$

with the notations $\vec{J}$ for the angular momentum, $\vec{N}$ for the random torque and β for the friction coefficient and assuming $\vec{N}(t)$ to have a Gaussian distribution and an infinitely short correlation time:

$$\vec{N}(t) = \vec{N}_0 \cdot \delta(t); \quad \langle \vec{J}(0) \cdot \vec{N}(t) \rangle = 0. \tag{2.21}$$

The solution of this equation is represented by

$$\Phi_J(t) = \langle \vec{J}(0)\, \vec{J}(t) \rangle = \langle \vec{J}(0)^2 \rangle \cdot e^{-\beta t}. \tag{2.22}$$

According to Doob's theorem [7, 8] the exponential decay of $\Phi_J(t)$ defines the process as *Gaussian–Markoffian*. The Gaussian distribution of $\Phi_J(t)$ is induced by the one of $\vec{N}(t)$. The infinite correlation time of $\vec{N}(t)$ is responsible for the Markoffian character of the process: Any value of $\vec{J}(t)$ after the time t_0 is independent of all events before the time t_0. Obviously equation (2.22) violates the conditions (2.15) and (2.16). Moreover the introduction of the constant friction coefficient β presupposes [15, 16, 17] the existence of a time t_0 which fulfils the condition

$$\tau_{\text{coll}} \ll \tau_0 \ll 1/\beta \tag{2.23}$$

where τ_{coll} indicates the time between subsequent collisions of a particle and $1/\beta$ represents a macroscopic time [15]. Equation (2.22) may be considered as a first approximation for the motion of a very heavy particle in a bath of very light molecules whose moments of inertia can be neglected [15].

The meaning of τ_0 can be understood with the aid of the *generalized Langevin equation* [11]:

$$\frac{d}{dt}\vec{J}(t) = -\int_0^t K(t-\tau)\cdot\vec{J}(\tau)\cdot d\tau + \vec{N}(t) \tag{2.24}$$

with the only assumptions

$$\langle\vec{N}(t)\rangle = 0 \quad \text{and} \quad \langle\vec{J}(0)\,\vec{N}(t)\rangle = 0. \tag{2.25}$$

Consequently the *correlation function* $\Phi_J(t)$ obeys

$$\frac{d}{dt}\Phi_J(t) = -\int_0^t K(t-\tau)\cdot\Phi_J(\tau)\cdot d\tau \tag{2.26}$$

and the *memory function* $K(t)$ equals the autocorrelation function of the random torque:

$$K(t) = \langle\vec{N}(0)\cdot\vec{N}(t)\rangle. \tag{2.27}$$

For memory functions $K(t)$ *characterized by a correlation time* τ_0:

$$\left.\begin{aligned} K(t) &\neq 0 \quad \text{for } 0 \leqq t \leqq \tau_0 \\ K(t) &= 0 \quad \text{for } t > \tau_0 \end{aligned}\right\} \tag{2.28}$$

the solution of the above equation of $\Phi_J(t)$ for $t > t_0$ is

$$\Phi_J(t) = \Phi_J(\tau_0)\, e^{-\beta(t-\tau_0)} \tag{2.29}$$

with β determined by

$$\beta = \int_0^{\tau_0} K(\tau)\cdot e^{\beta\tau}\cdot d\tau. \tag{2.30}$$

If $\tau_0 \ll 1/\beta$ this equation is approximated by

$$\begin{aligned} \beta &= \int_0^{\tau_0} K(\tau)\cdot d\tau = \int_0^{\infty} K(\tau)\, d\tau \\ &= \left(\int_0^{\infty} \Phi_J(\tau)\cdot d\tau\right)^{-1} = 1/T. \end{aligned} \tag{2.31}$$

If conditions (2.23), (2.28) are fulfilled, the correlation function $\Phi_J(t)$ can consequently be separated into *a microscopic and a hydrodynamic component* as suggested by Onsager [15]:

$$\left.\begin{aligned} \Phi_J(t) &= \Phi_{J,m}(t) + \Phi_{J,h}(t) \\ \Phi_{J,m}(t) &\cong 0 \quad \text{for } t > \tau_0 \\ \Phi_{J,h}(t) &= \Phi_J(\tau_0)\, e^{-\beta(t-\tau_0)}. \end{aligned}\right\} \tag{2.32}$$

Hitherto only one system has been rigorously investigated under these aspects: the heavy particle in a harmonic chain [17]. To find the *general solution* of equation (2.26) we introduce the new functions:

$$\Psi(t) = \frac{d}{dt}\Phi_J(t) \quad \text{and} \quad \Gamma(t) = \int_0^t K(t')\,dt'. \tag{2.33}$$

We can relate them by a convolution type Volterra equation of the second kind:

$$0 = \Psi(t) + \Gamma(t) + \int_0^t \Psi(t')\,\Gamma(t-t')\,dt'. \tag{2.34}$$

With the aid of [18] we find the solution:

$$\Psi(t) = -\Gamma(t) + \sum_{m=0}^{\infty} (-1)^m \underbrace{\Gamma(t) * \Gamma(t) ** \Gamma(t)}_{(2+m)\text{ ``factors''}}. \tag{2.35}$$

Correlation functions $\Phi(t)$ related to *special memory functions* $K(t)$ are listed in Table 2.1.

Table 2.1
Examples of memory functions and their corresponding correlation functions.

$K(t)$	$\Phi(t)$
0	1
$K_0^{1/2}\cdot\delta(t)$	$e^{-K_0^{1/2}t}$
K_0	$\cos(K_0^{1/2}\cdot t)$
$K_0\cdot e^{-\alpha t}$	$\frac{1}{2}\left(1-\frac{\alpha}{(\alpha^2-4K_0)^{1/2}}\right)\cdot e^{-(t/2)(\alpha+(\alpha^2-4K_0)^{1/2})}$ $+\frac{1}{2}\left(1+\frac{\alpha}{(\alpha^2-4K_0)^{1/2}}\right)\cdot e^{-(t/2)(\alpha-(\alpha^2-4K_0)^{1/2})}$ if $\alpha^2-4K_0\neq 0$ $\left(1+\frac{\alpha}{2}t\right)\cdot e^{-(\alpha\cdot t)/2}$ if $\alpha^2-4K_0=0$
$K_0 e^{-\alpha t}\cdot\cos\Omega t$	$A_1\cdot e^{-\gamma_1 t}+A_2\cdot e^{-\gamma_2 t}+A_3 e^{-\gamma_3 t}$ $A_1+A_2\cdot t\cdot e^{-\gamma_1 t}+A_3 e^{-\gamma_3 t}$ $[A_1\cos\omega t+A_2\sin\omega t]\cdot e^{-\gamma_1 t}+A_3\cdot e^{-\gamma_3 t}$ — $A_1, A_2, A_3, \gamma_1, \gamma_2, \gamma_3, \omega$ determined by cubic equations

As Wang and Uhlenbeck [19] pointed out, every *non-Markoffian* process can be considered as the result of a higher-order Markoffian process. E.g. if $\Phi_J(t)$ is non-Markoffian, $K(t)$ could be Markoffian. Indeed the $\Phi_J(t) = \langle\vec{J}(0)\cdot\vec{J}(t)\rangle$ corresponding to the Markoffian kernel [20]

$$K(t) = \langle\vec{N}(0)\,\vec{N}(t)\rangle = K_0\,e^{-\alpha t} \tag{2.36}$$

fulfils the requirements (2.15) and (2.16). If $4K_0 < \alpha^2$, $\Phi_J(t)$ is separable into a short-time and a long-time part (Table 2.1). The violation of conditions (2.15) and (2.16) has been transferred from the angular momentum correlation function $\Phi_J(t)$ to the correlation function $K(t)$ of the torques. The question now arises as to how many orders must be included to tolerate this violation? Although this question has not yet been answered, it seems to be primarily a matter of time scaling, the time scale being shortened by increasing the order of the correlation function.

2.4. *Short-time behaviour*

The general form of a correlation function determined by conditions (2.13), (2.15), (2.16) allows the following *series expansion near* $t = 0$:

$$\Phi(t) = \sum_{K=0}^{\infty} \frac{(-1)^k}{(2k)!} \cdot M_{2k} \cdot t^{2k}. \tag{2.37}$$

The coefficients M_{2k} can be related to the molecular dynamics [11, 21]. Considering linear molecules with the moment of inertia I, and

$$\langle \vec{J}^2 \rangle = 2IkT \qquad \langle \vec{N}^2 \rangle = \text{mean square torque}$$

$$\langle \vec{J}^4 \rangle = 8I^2(kT)^2$$

one finds the angular momentum correlation function [10]

$$\Phi_J(t) = \frac{\langle \vec{J}(0)\,\vec{J}(t) \rangle}{\langle \vec{J}(0)\,\vec{J}(0) \rangle} = 1 - \frac{\langle \vec{N}^2 \rangle}{\langle \vec{J}^2 \rangle} \cdot \frac{t^2}{2!} + \frac{\langle \vec{N}^2 \rangle^2}{\langle \vec{J}^2 \rangle^2} \frac{t^4}{4!} - + - \tag{2.38}$$

and its memory function

$$K_J(t) = \frac{\langle \vec{N}^2 \rangle}{\langle \vec{J}^2 \rangle} + \left[\left(\frac{\langle \vec{N}^2 \rangle}{\langle \vec{J}^2 \rangle} \right)^2 - \frac{\langle \vec{N}^2 \rangle}{\langle \vec{J}^2 \rangle} \right] \frac{t^2}{2!} - + -. \tag{2.39}$$

On the other hand the angular correlation function $\Phi_u(t)$ of the molecule fixed unit vector $\vec{u}$ can be expanded as

$$\Phi_u(t) = \langle \vec{u}(0)\,\vec{u}(t) \rangle = 1 - \frac{\langle \vec{J}^2 \rangle}{I^2} \frac{t^2}{2!} + \left[\frac{\langle \vec{J}^4 \rangle}{I^4} + \frac{\langle \vec{N}^2 \rangle}{I^2} \right] \frac{t^4}{4!} - + \tag{2.40}$$

and the corresponding normalized memory function as

$$K'_u(t) = K_u(t)/K_u(0) = 1 - \left[\frac{\langle \vec{J}^2 \rangle}{I^2} + \frac{\langle \vec{N}^2 \rangle}{\langle J^2 \rangle} \right] \frac{t^2}{2!} - + - + \tag{2.41}$$

with $K_u(0) = \langle \vec{J}^2 \rangle / I^2$. Thus M_2 of $\Phi_u(t)$ is independent of any interaction.

By comparing the expressions (2.38–2.39) and (2.40–2.41) one finds two interesting features:

i) In a system of molecules with extremely weak interaction $\Phi_J(t)$ is a constant, whereas $\Phi_u(t)$ and $K_u(t)$ decay. This decay is due to the thermal distribution of the $\vec{J}(t)$. It implies the assumption of small interactions necessary for the thermalization.

ii) In a system with strong interactions

$$\langle N^2\rangle \gg (\langle \vec{J}^2\rangle)^2 I^{-2} = 4(kT)^2 \tag{2.42}$$

the normalized angular memory function $K'_u(t)$ approaches the momentum correlation function $\Phi_J(t)$ at least for short times [11]. According to the computer model calculations by Berne et al. [11] on liquid CO this seems to be also valid for longer times. Yet no rigorous proof exists.

2.5. *Quantum mechanical correlation functions*

The quantum mechanical correlation function [3, 4] corresponding to the classical $\Phi_u(t)$:

$$C_u(t) = \langle \vec{u}(0)\, \vec{u}(t)\rangle_{\mathrm{qm}} \tag{2.43}$$

is *complex* and obeys the *symmetry relation*

$$C_u(-t) = C_u^*(t). \tag{2.44}$$

The *symmetrization* of this correlation function yields a real and even function:

$$C_{u,s}(t) = \langle\{\vec{u}(0)\, \vec{u}(t)\}\rangle_{\mathrm{qm}} = C_{u,s}(-t). \tag{2.45}$$

According to Schofield [22] or Egelstaff [23] $C_u(t)$ can be *approximated* by the classical correlation function with the aid of a complex argument:

$$C_u(t) \cong \Phi_u\left(t - \frac{i}{2}\frac{\hbar}{kT}\right) \tag{2.46}$$

or

$$C_u(t) \cong \Phi_u\left(\left(t^2 - i\frac{\hbar}{kT}t\right)^{1/2}\right). \tag{2.46}$$

Using the second approximation by Egelstaff we find for the real and imaginary part of $C_u(t)$:

$$\mathrm{Re}\, C_u(t) = C_{u,s}(t) \cong 1 - \left[\frac{M_2}{2!} + \frac{\hbar^2}{(kT)^2}\frac{M_4}{4!}\right]t^2 + \left[\frac{M_4}{4!} + \frac{\hbar^2}{(kT)^2}\frac{M_6}{6!} + \frac{\hbar^4}{(kT)^4}\frac{M_8}{8!}\right]t^4 \tag{2.47}$$

$$\mathrm{Im}\, C_u(t) \cong \frac{\hbar}{kT}\frac{M_2}{2!}t - \left[\frac{\hbar}{kT}\frac{M_4}{4!} + \frac{\hbar^3}{(kT)^3}\frac{M_6}{6!}\right]t^3. \tag{2.48}$$

For a linear molecule the coefficient M'_2 of $t^2/2!$ in $C_{u,s}(t)$ is

$$M'_2 = \frac{kT}{I} + \frac{1}{3}\frac{\hbar^2}{I^2} + \hbar^2\frac{\langle \vec{N}^2\rangle}{24I^2(kT)^2} \tag{2.49}$$

in agreement with the result obtained by Nienhuis [24]. Hence if

$$kT \gg \hbar^2/3I \quad \text{and} \quad (kT)^2 \gg \langle \vec{N}^2 \rangle/24 \tag{2.50}$$

the $C_{u,s}(t)$ approaches $\Phi_u(t)$.

3. Angular Autocorrelation Functions and Vibration-Rotation Spectra

3.1. *Basic relations*

Each infrared active vibrational transition $i \to f$ of a molecule involves an electric transition dipole moment $\vec{\mu}_{if}$ oscillating with the frequency ω_{if}. As the molecule rotates, the direction of $\vec{\mu}_{if}$ varies and modulates the spatial component $(\vec{e}_k \cdot \vec{\mu}_{if})$. This modulation gives rise to the discrete rotational structure of the vibrational absorption in the gas phase (Fig. 3.1). In a dense medium the rotational structure converts to a continuous line shape (Fig. 3.1) and its interpretation in terms of rotational energy levels is obscured.

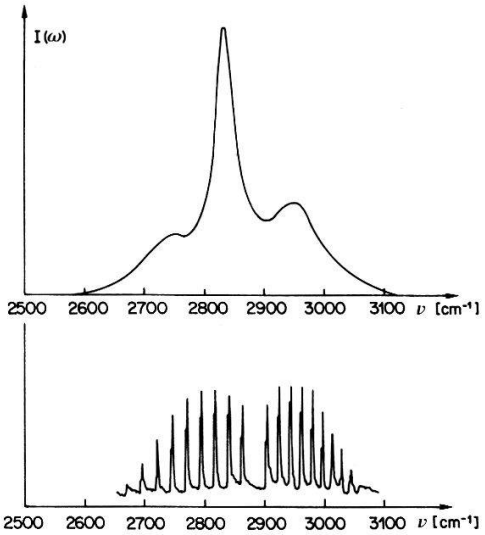

Figure 3.1
Vibration-rotation spectra of gaseous HCl and of HCl dissolved in CCl_4 at room temperature.

However, *linear response theory relates the line shape to the autocorrelation function* [14]:

$$C_s'(t) = \langle \{(\vec{e}_k \vec{\mu}_{if}(0))(\vec{e}_k \vec{\mu}_{if}(t))\} \rangle_{\mathrm{qm}}$$

$$= 2 \int_{-\infty}^{+\infty} \chi''(\omega' + \omega_{if}) \frac{E_T(\omega' + \omega_{if})}{(\omega' + \omega_{if})} \cos(\omega' + \omega_{if})\, d\omega'. \tag{3.1}$$

This expression represents a quantum mechanical analogue to equation (2.11). $\vec{e}_k$ indicates the direction of the electric field of the radiation and $E_T(\omega)$ the average thermal energy of the harmonic oscillator (3.4)

$$E_T(\omega) = \tfrac{1}{2}\hbar\omega \cdot \coth \frac{\hbar\omega}{2kT}. \tag{3.2}$$

The measured absorption coefficient $\alpha(\omega)$ is related to the imaginary part $\chi''(\omega)$ of the susceptibility

$$\chi''(\omega) = c \frac{n(\omega)}{\omega} \alpha(\omega) \tag{3.3}$$

where $n(\omega)$ is the real part of the refraction index.

In the near infrared, the inequality

$$\hbar(\omega' + \omega_{if}) \gg kT \tag{3.4}$$

induces

$$E_T(\omega' + \omega_{if}) \cong \tfrac{1}{2}\hbar(\omega' + \omega_{if}) \tag{3.5}$$

yielding

$$C_s'(t) = \int_{-\infty}^{+\infty} \frac{\alpha(\omega' + \omega_{if})}{(\omega' + \omega_{if})} \cos(\omega' + \omega_{if})\, t\, d\omega'$$

$$= \int_{-\infty}^{\pm\infty} I(\omega' + \omega_{if}) \cos(\omega' + \omega_{if})\, t\, d\omega'. \tag{3.6}$$

With respect to

$$\vec{\mu}_{if}(t) = \vec{u}_{if}(t) \cdot \mu_{if}(t) \cos \omega_{if} t \quad \text{with } |\vec{\mu}_{if}(t)| = 0, \quad \text{and } |\vec{u}_{if}(t)| = 1 \tag{3.7}$$

$C_s'(t)$ is influenced by three different processes: the high-frequency oscillation ω_{if}, the vibrational relaxation $\langle \mu_{if}(0)\, \mu_{if}(t) \rangle$ and the rotational relaxation

$$\langle (\vec{e}_k \vec{u}_{if}(0))\, (\vec{e}_k \vec{u}_{if}(t)) \rangle.$$

The influence of the oscillation can be eliminated by a Fourier transformation relative to the shifted band centre ω_{if}, whereas in principle the experimental infrared data do not allow the separation of vibrational and rotational relaxation [81]. However, the vibrational relaxation functions determined experimentally by Lauberau [82] with laser techniques and by Konynenburg [83] with Rayleigh scattering usually show an exponential decay with time constants of a few picoseconds. Therefore most $C_s'(t)$ can be normalized for short times:

$$C_{u,s}(t) = \langle \{ (\vec{e}_k \vec{u}_{if}(0))\, (\vec{e}_k \vec{u}_{if}(t)) \} \rangle$$

$$= \int_{\text{band}} I(\omega') \cos \omega' t\, d\omega' \Big/ \int_{\text{band}} I(\omega')\, d\omega' \tag{3.8}$$

which yields an approximate, symmetric rotational correlation function. For isotropic surroundings of rotating molecules the averaging over all orientations $\vec{e}_k$ of the polarization results in

$$C_{u,s}(t) = \langle \{ \vec{u}_{if}(0)\, \vec{u}_{if}(t) \} \rangle. \tag{3.9}$$

Finally we have to mention that according to Gordon [21] the coefficients M_{2k} of the series expansions in Section 2.4 correspond to the spectral moments:

$$M_{2k} = \int_{\text{band}} \frac{\alpha(\omega_{if} + \omega')}{(\omega_{if} + \omega')} \cdot \omega'^{2k} \cdot d\omega' \Big/ \int_{\text{band}} \frac{\alpha(\omega_{if} + \omega')}{(\omega_{if} + \omega')}\, d\omega'. \tag{3.10}$$

3.2. *Physical limitations*

Some of the implicit assumptions inherent to the evaluation of correlation functions from experimental spectra have to be emphasized:

i) The *wavelength of infrared radiation* is considerably larger than the molecular dimensions. Thus the correlation functions measured correspond to domains of molecules and require, in principle, the inclusion of interference terms between the molecules of the domain [5]. This is particularly true for correlation functions determined from pure rotation spectra. Fortunately the vibrational states of neighbouring molecules can be assumed to be uncorrelated with respect to the phase in liquids which allows the average of the individual correlation functions to be measured. In molecular crystals however, vibronic coupling between adjacent molecules is possible and may obscure the physical meaning of $\Phi_u(t)$.

ii) The *average shape of the molecule* generally depends on the vibrational states i and f, this leads to different moments of inertia I_i and I_f as well as to different intermolecular forces. Because this effect is caused by anharmonicity the lowest vibrational transitions should be investigated [25].

iii) The *transition frequency* ω_{if} is usually shifted by molecular interactions. Since errors in the choice of ω_{if} in equation (3.7) induce serious phase shifts in the correlation function $C_{u,s}(t)$ special methods had to be developed for its determination (Section 3.3).

iv) *Hot bands* corresponding to the vibrational transitions from higher states may distort the band shape of the transitions from the ground states. In the near infrared the thermal occupation factor suppresses the hot bands at room temperatures.

v) During molecular collisions dipole moments may be induced by multipole interactions. They give rise to a weak and very broad absorption. Fortunately the *collision induced absorption* appears in the far infrared as demonstrated for liquid H_2 and N_2 [26].

vi) Because the determination of the correlation function requires a Fourier transform over the whole band, *overlapping absorption lines* are excluded. This usually restricts the method to small molecules. The method can be extended to complex molecules if there exists at least one well-separated transition. However, this raises the problem of relating the motion of the transition dipole to that of the entire molecule.

3.3. *Experimental evaluation of autocorrelation and memory functions*

$C_{u,s}(t)$ is determined from the measured absorption profile

$$\hat{I}(\omega_{if}+\omega') = \frac{\alpha(\omega_{if}+\omega')}{(\omega_{if}+\omega')} \Bigg/ \int_{\text{band}} \frac{\alpha(\omega_{if}+\omega')}{(\omega_{if}+\omega')}\, d' \tag{3.11}$$

by the full cos-transform

$$C'_{u,s}(t) = \int_0^\infty \hat{I}_s(\omega) \cos \omega t \, d\omega \tag{3.12}$$

With the symmetrized band shape

$$\hat{I}_s(\omega) = \hat{I}_s(\omega_{if} + \omega') = \tfrac{1}{2}(\hat{I}(\omega_{if} + \omega') + \hat{I}(\omega_{if} - \omega')) = \tfrac{1}{2}(1 + e^{\hbar\omega'/kT})\, I(\omega_{if} + \omega'). \tag{3.13}$$

$C'_{u,s}(t)$ can be expressed as

$$C'_{u,s}(t) = \mathrm{Re}\, e^{i\omega_{if}t}\left[\int_{\omega_{if}} \hat{I}_s(\omega)\cos\omega t\, d\omega + i \int_{\omega_{if}} I_s(\omega)\, th\left(\frac{\hbar\omega}{2kT}\right)\sin\omega t\, d\omega\right]. \tag{3.14}$$

Because an absorption band usually does extend over a spectral region larger than 300 cm^{-1} the second integral is small at temperatures above 200°K. Its main contribution lies at times shorter than about 10^{-14} sec. For longer times the second integral can be neglected, which yields

$$C'_{u,s}(t) \cong \cos\omega_{if} t \int_{\text{band}} \hat{I}(\omega_{if} + \omega')\cos\omega' t\, d\omega'$$

$$\cong \cos\omega_{if} t \cdot C_{u,s}(t). \tag{3.15}$$

Hence a *precise value of* ω_{if} can be determined from the mean period of $C'_{u,s}(t)$.

For the *evaluation of* ω_{if} *from broad bands* measured at low temperatures another procedure is recommended. Since the derivative of $\hat{I}_s(\omega)$ vanishes at ω_{if} the $\hat{I}(\omega_{if})$ satisfies the relation

$$\frac{d\hat{I}}{d\omega}(\omega_{if}) = \frac{\hbar}{kT}\hat{I}(\omega_{if}); \tag{3.16}$$

ω_{if} is determined by numerical substitution in the above equation. The result is checked by performing the sin-transforms of $\hat{I}(\omega)$ and $\hat{I}(\omega_{if} + \omega')$.

Another problem concerns the *choice of the integration limits* $w'_{\min}$ and $\omega'_{\max}$. According to equation (2.40) the second moment M_2 is given by

$$M_2 = kT/I$$

for linear molecules in the classical approximation. Occasionally this relation was used to numerically determine the integration limits [25]. Unfortunately the moments of inertia of a molecule in a dense medium and in a gas may differ. In addition, for strong molecular interactions the above relation must be corrected according to equation (2.49). For this reason we determine the zero-absorption level and the related $\omega'_{\min}$ and $\omega'_{\max}$ by numerical extrapolation from the parts far outside the wings of the absorption band.

For the *numerical transformation of the measured spectrum* the frequency has to be digitalized into equidistant steps $\Delta\omega$. This approximation modifies the proper correlation function to a periodic function with the period $\tau = 2\pi/\Delta\omega$. The calculated correlation function is therefore only reliable up to times $\pi/\Delta\omega$. The spectral resolution $\Delta\omega_{sp}$ of the spectrometer limits the minimal value of $\Delta\omega$ to

$$\Delta\omega \geqslant 2\Delta\omega_{sp}.$$

E.g., for the Beckman IR 12 spectrometer the *time range* is restricted to $t \leqslant 1.6 \cdot 10^{-11}$ s.

The *time resolution* for the determination of $C_{u,s}(t)$ is given by the width of the studied band shape. If the experimental data expand from $\omega_{if} - \omega_L$ to $\omega_{if} + \omega_L$, the time resolution Δt is restricted by

$$\Delta t \geqq \pi/\omega_L.$$

As an example the broad band of HCl in CCl_4 (Section 4) with $\omega_L = 300\ \mathrm{cm}^{-1}$ allows a time resolution of $\Delta t \geqq 0.5 \cdot 10^{-13}$ s.

As shown in Section 2.3 the *memory function* $K_u(t)$ is of basic interest. Thus we evaluated $K_u(t)$ numerically from the integro-differential equation (2.26) by:

$$-K_u(0) = \frac{d^2}{dt^2} C_{u,s}(t)\Big|_{t=0}$$

$$-K_u(n\Delta t) = 2 \sum_{m=1}^{n-1} K((n-m)\,\Delta t)\, C_{u,s}(m\Delta t) + K_u(t)\, C_{u,s}(n\Delta t) + \frac{2}{\Delta t}\frac{d}{dt} C_{u,s}(n\Delta t). \tag{3.17}$$

The differentiation is performed by the usual Lagrange formalism with relatively high precision. Unfortunately the form of the integro-differential equation forbids the application of integration algorithms more sophisticated than the trapezoidal rule. With the choice of time steps $\Delta t \leqslant 0.5 \cdot 10^{-14}$ s the stability range of $K_u(t)$ was brought to about 10^{-12} s. The stability of this numerical procedure was checked by varying Δt.

4. Experimental Correlation Functions of Diatomic Molecules in Liquids

4.1. *Introduction*

The molecular motion in liquids can be studied by the determination of the correlation functions either of *molecules of pure liquids or of small molecules dissolved in liquids*. Diatomic molecules are well suited for the latter. As probes they yield information on the structure of the holes in the host liquid [27–29]. Moreover the interpretation of the correlation functions of diatomic molecules is straightforward. In comparison the understanding of the correlation functions related to more complex molecules demands additional computations (Section 6).

For some years it has been known in infrared spectroscopy that the *vibration-rotation spectra of diatomic molecules* (HCl, HBr) dissolved in simple liquids (CCl_4, CS_2) display structures indicating almost free rotation (Fig. 3.1) [30, 31]. The many attempts to derive the parameters of motion from the continuous spectra had only limited success. Therefore we applied the correlation function method to this problem.

In addition these liquids represent the *opposite of the model systems adapted to the Langevin equation*. The probe molecules are much lighter than their neighbouring host molecules. Because of the relatively large cavities in the liquids, the time interval between collisions equals or exceeds the duration of the collisions. The force fields acting on a probe molecule are weak due to the high symmetry of the host molecules and their strong covalent bonds.

In order to avoid confusion arising from steric effects the investigation was restricted to *liquid tetrachlorides*: CCl_4, $SiCl_4$, $TiCl_4$, $GeCl_4$, $SnCl_4$ [28, 29]. This essentially varied the cavity size of the liquid.

HCl, DCl and CO, whose data [32] are listed in Table 4.1, were selected as *probe molecules*. The data of the tetrachlorides [33] are summarized in Table 4.2.

Table 4.1
Properties of HCl, DCl and CO.

	Mass	Moment of inertia, I [10^{-40} cgs]	Bond length [Å]	$\tilde{\nu}_{0\to1}$ [cm^{-1}]
HCl	36.47	2.65	1.275	2885
DCl	37.47	5.16	1.275	2040
CO	26	14.3	1.128	2170

4.2. *Interpretation of the correlation functions*

To start we describe the *correlation functions of diatomic gases* (e.g. Fig. 4.2). The correlation functions drop to a minimum below zero indicating an almost complete reversion of the initial direction of the molecules, and they approach zero for long times.

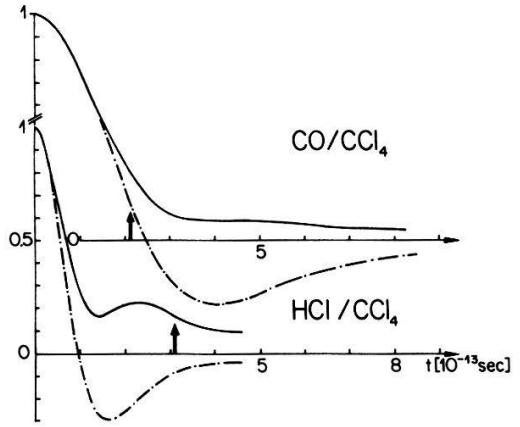

Figure 4.1
Angular autocorrelation function $\Phi_u(t)$ of HCl and CO: —— dissolved in CCl_4, ----- gas. The arrows indicate the value of the mean time of flight.

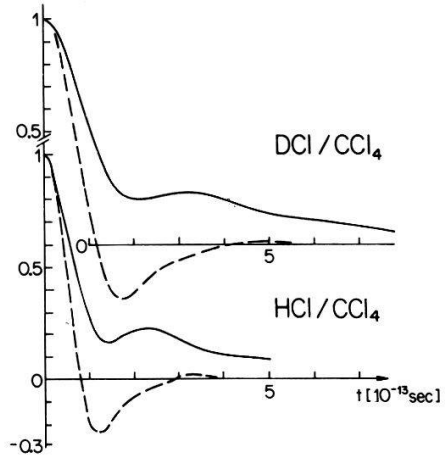

Figure 4.2
Angular autocorrelation functions $\Phi_u(t)$ (——) and normalized memory functions $K'(t)$ (-----) of HCl and DCl dissolved in CCl_4 at room temperature. The arrows indicate the value of the mean time of flight.

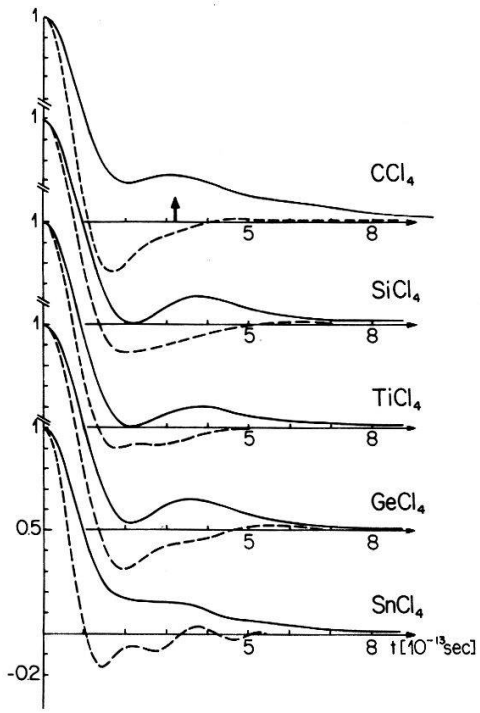

Figure 4.3
Angular autocorrelation functions $\Phi_u(t)$ (——) and normalized memory functions $K'(t)$ (-----) of DCl in the tetrachlorides at room temperature.

The *correlation functions of HCl and DCl in the liquid tetrachlorides* are shown in Figures 4.2 and 4.3 and that of CO in CCl_4 in Figure 4.1. The *correlation function of HCl in CCl_4*, Figures 4.1, 4.2, 4.3, reveals the following features:

i) The variation of the average angle of rotation of HCl in CCl_4 is smaller than that of gaseous HCl.

ii) The minimum of the correlation function occurs at an earlier time τ_{min} than for the HCl gas.

iii) The minimum of the correlation function at τ_{min} is followed by a maximum at τ_{max}.

Feature i) and equation (2.40) give evidence for the existence of torques hindering the rotation of the diatomic molecule in the liquid. The magnitude and the fluctuation of the torques determine the deviation of the correlation function from the ideal-gas shape [6]. These torques are influenced by

i) the life-time of the cavity limited by the translational and rotational motions of the host molecules,

ii) the vibrations of the host molecules,

iii) the rattling frequency of the HCl in the cavity.

The rotational and translational motions of the CCl_4 molecules are slow due to the large mass and moment of inertia. Hence contribution i) can be neglected. The comparison of the correlation functions of HCl and DCl in CCl_4 in Figure 4.2 yield a precise *isotopic shift* proportional to $(I/kT)^{1/2}$ for times smaller or equal to τ_{min}. From this observation we conclude an *almost free rotation for times $t < \tau_{min}$*.

Table 4.2
Properties of the tetrachlorides

	Mass	Moment of inertia [10^{-40} cgs]	Bond length [Å]	Lowest transitions [cm^{-1}] δ_s	δ_a	ν_s	ν_a	r (circumscribed sphere) / r (central atom)
CCl_4	153.8	520	1.76	217	313	459	760	4.62
$SiCl_4$	169.8	640	2.02	150	220	425	607	3.18
$TiCl_4$	189.7	760	2.21	120	144	385	496	2.95
$GeCl_4$	214.4	660	2.08	132	171	397	451	3.18
$SnCl_4$	260.5	850	2.30	105	132	368	403	2.75

Table 4.3
Parameters of the motion of DCl and HCl in their cavities. The cavity diameter for CCl_4 is calculated according to reference [34] and those for the other tetrachlorides are derived from the corresponding τ_{max}.

	τ_{max} [10^{-13} s]		τ_{min} [10^{-13} s]		Isotopic shift	Range of τ_{vibr} [10^{-13} s]		$\langle N^2\rangle^{1/2}$	Cavity, ϕ [Å]	
	HCl	DCl	HCl	DCl	$\tau_{min}^{HCl}/\tau_{min}^{DCl} = 1.4$	min	max	[10^{-14} cgs]	DCl	HCl
CCl_4	2.40	3.1	1.43	2.05	1.43	0.44	1.5	9.1 ± 0.9	4.4	4.4
$SiCl_4$	3.0	3.8	1.5	2.2	1.48	0.55	2.2	6.4 ± 0.7	5.4	5.5
$TiCl_4$	2.8	3.8	1.43	2.15	1.50	0.67	2.75	6.5 ± 0.7	5.4	5.14
$GeCl_4$	2.5	3.55	1.59	2.15	1.35	0.74	2.5	7.2 ± 0.8	5.0	4.6
$SnCl_4$	2.1	3.05	1.4	2.9	2.07	0.83	3.7	8.1 ± 0.8	4.3	3.8

However, the half periods τ_{vibr} of the four ground state vibrations are in the range of interest (Tables 4.2 and 4.3):

$$0.44 \cdot 10^{-13}\ \text{s} < \tau_{vibr} < 1.5 \cdot 10^{-13}\ \text{s}.$$

Fortunately, Narten et al. [34] investigated liquid CCl_4 by x-ray scattering and succeeded in constructing a *lattice model of the average liquid structure*. In this model the cavities are approximately octahedral with chlorine atoms at the corners (Fig. 4.4). Introducing the average velocity $\bar{v}$ of the HCl molecule:

$$\bar{v}^2 \simeq \overline{v^2} = 3kT/m \tag{4.1}$$

and the cavity diameter d, we can deduce a mean time of flight of the HCl between the *collisions with the walls*:

$$\tau_{tr} = d/\bar{v} \tag{4.2}$$

in the range

$$1.8 \cdot 10^{-13}\ \text{s} < \tau_{tr} < 3.1 \cdot 10^{-13}\ \text{s}.$$

In the time domain near $\tau_{tr} \gtrsim \tau_{max}$ collisions with the wall occur and interrupt the motion. Between the collisions, $t < \tau_{max}$ the rotation of the HCl is only slightly disturbed

by weak fields within the cavity. This hypothesis is supported by the *correlation function of CO in CCl_4* (Fig. 4.1). The size of CO is not very different from that of HCl (Fig. 4.4) in agreement with

$$1.6 \cdot 10^{-13}\ \text{s} < \tau_{\text{trans}} < 2.10^{-13}\ \text{s}.$$

However, the moment of inertia is much larger. Therefore the CO rotates through a much smaller angle between the successive wall to wall collision. The period of almost free rotation is too short for a distinct minimum of the correlation function (Fig. 4.1).

In considering the *other tetrachlorides*, increasing the size of the central atom (Table 4.2) causes the structure of the tetrachlorides to become more open allowing a denser packing. This results in a reduction of the mean time of flight τ_{tr}. On the other side the vibrational modulation of the torques slows down (Table 4.3). The lower limit of τ_{vibr} corresponding to the stretch vibration is smaller than τ_{min} whereas the upper limit related to a deformation vibration lies above τ_{max}.

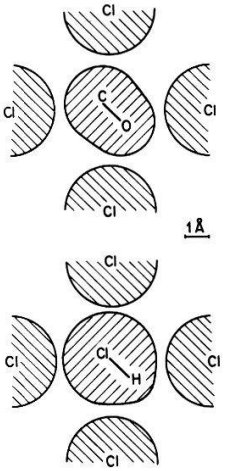

Figure 4.4
Cavities in liquid CCl_4 occupied by HCl and CO molecules respectively.

These qualitative arguments do not allow a rigorous description. Yet from the experimental correlation functions it follows that the cavity diameter determines the molecular motion for times $t > \tau_{\text{min}}$ and the torques within the cavity for times $\tau \lesssim \tau_{\text{min}}$. On this basis we conclude the cavity diameter in $SnCl_4$ to be considerably smaller than in CCl_4 while for $GeCl_4$ to lie in between. At first glance, inconsistent with this model, $SiCl_4$ and $TiCl_4$ show more pronounced minimas and maximas of the correlation function. However, the study of $SiCl_4$ by x-ray scattering [35] and of $SiCl_4$ and $TiCl_4$ by high resolution Raman spectroscopy [36] provided evidence for the *existence of dimers* in the liquid. The dimers cause larger holes in the liquids and thus increase the time τ_{tr} between the wall collisions of the diatomic molecules. They also diminish the mean torques acting within the cavity in agreement with our experimental results: smaller mean square torques and larger cavity diameters for $SiCl_4$ and $TiCl_4$ than for the other tetrachlorides (Table 4.3).

4.3. *Memory functions*

For all experimentally determined memory functions $K_u(t)$ of the diatomic molecules in the tetrachlorides the main variation is observed to occur during the time τ_{tr} between the wall collisions. This variation is mainly caused by the torques within

the cavity. At the times τ_{max} corresponding to the wall collisions, $K_u(t)$ rapidly drops to zero reflecting the *memory destroying effect of wall collisions*. The oscillating structure of the $K_u(t)$ for $TiCl_4$, $GeCl_4$ and $SnCl_4$ seems to mirror the oscillation of the intermolecular fields due to the ground state vibrations of the host molecules.

For additional information on $K_u(t)$ the *mean square torques* $\vec{N}^2$ were determined from the band shapes (Table 4.3) according to equations (2.38) and (3.10). The introduction of these data into inequality (2.42) demonstrates the $\langle \vec{N}^2 \rangle$ to be almost equal to $4(kT)^2$. Therefore $K_u(t)$ must not be interpreted as the angular momentum correlation function $\Phi_J(t)$.

4.4. *Long-time behaviour of the correlation and memory functions*

Finally consider the long-time behaviour of the measured correlation and memory functions on the basis of Section 2.2. As an example, the logarithmic plot of $\Phi_u(t)$ of

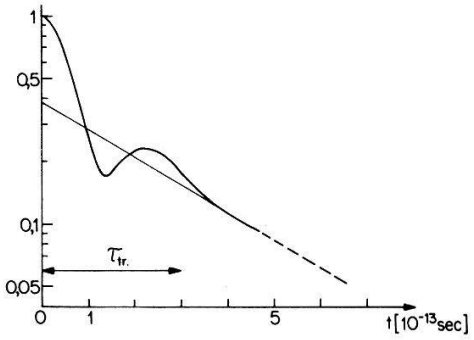

Figure 4.5
Semilogarithmic plot of the angular autocorrelation function $\Phi_u(t)$ of HCl dissolved in CCl_4. The exponential approximation for $t > 4 \cdot 10^{-13}$ s is given by (-----) $\Phi_u(t) \simeq 0.38\, e^{-t/3.3\ 10^{-13}s}$.

HCl in CCl_4 in Figure 4.5 exhibits an exponential decay at times larger than $4 \cdot 10^{-13}$ s, i.e. after a few wall collisions. It can be approximated by

$$\Phi_u(t > 4 \cdot 10^{-13}\ \text{s}) = B\, e^{-t/t_0}, \quad B = 0.38, \quad t_0 = 3.3 \cdot 10^{-13}\ \text{s}.$$

Hence the long-time component of the correlation function shows an astonishingly short relaxation time t_0. The onset of the exponential decay at $4 \cdot 10^{-13}$ s agrees well with the fact that $K_u(t)$ simultaneously approaches zero.

5. Diatomic Impurities in Alkalihalides

5.1. *Introduction*

Diatomic ions in alkalihalides have attracted considerable interest in the past ten years [37–51]. Usually they occupy the site of an anion in the fcc host lattice. The fields acting on the ions in the alkalihalides are far stronger than on molecules in liquids or molecular crystals presenting new features in the microdynamics which require further investigation. Since the determination of angular correlation functions from vibration-rotation spectra is not bound to low temperatures it adds new information on this problem. From the point of view of correlation functions these impurities are of special interest the strong crystalline fields allowing the approximate evaluation of the angular momentum correlation function $\Phi_J(t)$ according to Section 2.3.

For reference we summarize the latest data on OH^- and OD^- in alkalihalides obtained by different methods:

Infrared

Stretching vibrations at $\omega_0 = 3600$–$3700\ cm^{-1}$ for OH^- and $\omega_0 = 2600$–$2700\ cm^{-1}$ for OD^- [40–42].

Sidebands at $\omega_0 + \omega_{libr}$ with $\omega_{libr} = 250$–$350\ cm^{-1}$ for OH^- and $\omega_{libr} = 170$–$230\ cm^{-1}$, attributed to a two-dimensional libration in accordance with the isotopic shift of ω_{libr} [40–42].

Sidebands at $\omega_0 + \omega_{nD}$ with $\omega_{nD} = 10$–$30\ cm^{-1}$ [41], incompatible with the Devonshire model of an octahedral potential and thus labelled non-Devonshire.

Far infrared

Direct observation of ω_{libr} and ω_{nD} [39, 43–45].

Microwaves

Resonances at $\omega_{mw} = 0.1$–$1\ cm^{-1}$ indicating a local C_{4v} symmetry [47].

Field and stress induced dichroism

Observations in the infrared and in the ultraviolet [37, 38, 42, 43].

Thermal conductivity

Indication of a strong phonon scattering at temperatures corresponding to ω_{nD} [46].

5.2. *The two-dimensional off-centre librator model*

The experimental facts mentioned in the foregoing Section 5.1 and the temperature dependence of the correlation functions presented in Section 5.4 inspired our proposal of a simplified model of OH^- and OD^- in alkalihalides [52]. A more detailed discussion is given for clarity [53].

The microscopic situation is sketched in Figure 5.1. The important *features of the model* are:

i) The diatomic ions are considered to be dipoles with finite distance l between the centres of negative and positive charges.

ii) The centre of mass (cm) does not coincide with the centres of the charges. It is therefore not identical with the centre of interaction defined as the point whereupon the various forces act [53].

iii) There is a negative net charge $-e$.

To simplify the mathematical problem we restrict ourselves to *two dimensions* and a repulsive intermolecular potential of the Lennard–Jones 6–10 type. The multipole expansion of the potential $V(r, r_1, \alpha, \gamma)$

is given by:

$$V = \epsilon \sum_{n=0}^{\infty} \{\lambda r_1'^{2n}[P_{2n}(\cos\alpha) + P_{2n}(\sin\alpha)] - (1+\lambda)\, r'^{2n}[P_{2n}(\cos\gamma) + P_{2n}(\sin\gamma)]$$
$$+ \kappa r'^{2n}[C_{2n}^{(k/4)}(\cos\gamma) + C_{2n}^{(k/4)}(\sin\gamma)]\} \tag{5.1}$$

with the Legendre polynomials P_{2n} and the Gegenbauer polynomials $C_{2b}^{(\beta)}$ [54] and the abbreviations

$$r_1' = r_1/b, \quad r' = r/b, \quad \epsilon = \frac{2e^* e}{b}, \quad \kappa = \frac{C}{\epsilon b^k} \simeq \left(\frac{\sigma}{b}\right)^k,$$

where σ indicates the sum of the ionic radii and $k = 10$.

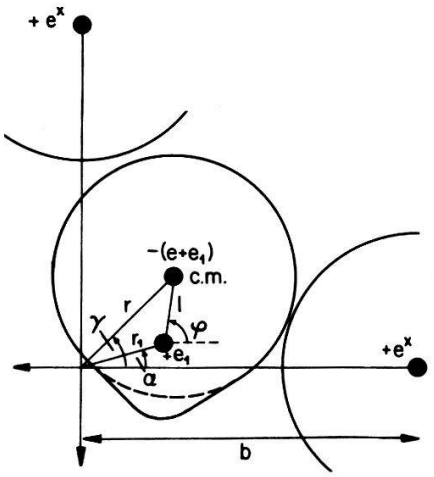

Figure 5.1
Parameters used in the two-dimensional off-centre librator model.

The lowest non-constant term is retained:

$$V_1 = \frac{\epsilon}{b^2}[\lambda l^2 - 2r\lambda l\cos(\phi - \gamma) + r^2(48\kappa - 1)]. \tag{5.2}$$

The next term is used only to specify the appropriate initial conditions corresponding to the potential minima for the solutions of the equations of motion:

$$\left.\begin{aligned} &M\ddot{r} - Mr\dot{\gamma}^2 + \frac{\epsilon}{b}(48\kappa - 1)\, r = \frac{\epsilon}{b^2}\lambda l(48\kappa - 1) \\ &I\ddot{\phi} + \lambda l \cdot \frac{\epsilon}{b^2} r \cdot \sin(\phi - \gamma) = 0 \\ &Mr^2\ddot{\gamma} + 2Mr\dot{r}\dot{\gamma} - \lambda l \frac{\epsilon}{b^2} r \cdot \sin(\phi - \gamma) = 0. \end{aligned}\right\} \tag{5.3}$$

They cannot be solved analytically. Thus we evaluated approximate solutions for high and low temperatures. Since the experimental results [37, 38, 42, 43] as well as the higher-order terms of V yield potential minima at specific directions of γ we assume

for low temperatures the ion to librate about its equilibrium position and suggest the approximations:

$$\ddot{\gamma} \sim 0 \qquad \sin(\phi - \gamma) \simeq \phi - \gamma = \chi \tag{5.4}$$

$$\left.\begin{aligned} & r(t) = r_0 + \delta_0 \cos(\omega_r t + \alpha); \quad r_0 = \frac{\lambda l}{48\kappa - 1} \quad \omega_r^2 = \frac{\epsilon(48\kappa - 1)}{Mb^2} \\ & \ddot{\chi}(t) + \chi(t) \frac{\epsilon\lambda l}{b^2}\left[\frac{1}{Mr(t)} + \frac{r(t)}{I}\right] = 0; \quad \omega_\chi^2 \simeq \frac{\epsilon \cdot \lambda l}{b^2}\left[\frac{1}{Mr_0} + \frac{r_0}{I}\right] \\ & \gamma(t) = \frac{at + b}{1 + \dfrac{I}{Mr^2(t)}} - \chi(t) \frac{I}{Mr^2(t)} \end{aligned}\right\} \tag{5.5}$$

with the integration constants α, δ_0. If the amplitude of the centre of mass oscillation $r(t)$ is small: $\delta_0 \ll r_0$ the second line becomes a Mathieu equation [55] of the canonical form

$$y'' + y(a - 2q\cos(2x)) = 0, \tag{5.6}$$

where

$$a(q) = \frac{4\epsilon\lambda l}{Ib^2\omega_r^2}(r_0 + \delta_0) + 2q \quad q = \frac{2\epsilon\lambda l\delta_0}{b^2\omega_r^2}\left[\frac{1}{Mr_0^2} - \frac{1}{I}\right]$$

characteristic for a two-dimensional librator. The linear term in $\gamma(t)$ can be eliminated by the appropriate choice of the starting conditions. This solution states the translational oscillation ω_r of the centre of mass about the off-centre equilibrium position r_0. Consequently the net charge $-e$ and the charge defect $+e$ at the lattice point give rise to an oscillating dipole moment. The corresponding resonance is attributed to the non-Devonshire line ω_{nD} in agreement with the strong phonon scattering observed in thermal conductivity [46] and the strong dependence on the lattice found by Bosomworth [43, 49]. We emphasize that ω_r must not be considered as a localized lattice vibration [56]. It is only due to the rotation-translation coupling caused by the missing coincidence of the centre of mass and the centre of interaction.

The approximate Mathieu equation represents the libration of the ion axis about the radius vector from the lattice point to the centre of mass.

The third equation reflects the variation of $\gamma(t)$ due to the combined libration ω_χ and the oscillation ω_r if a and b are properly chosen.

Thus the model represents the main features actually observed at low temperatures.

For the *high temperature* solution, assume a molecule with a thermal energy larger than the rotational barriers [57, 53] responsible for the low temperature behaviour. Hence it rotates as a whole about the lattice point with the off-centre position of the centre of mass mainly determined by the thermal energy and the repulsive part of the surrounding ion cores. The specific assumptions are

$$\ddot{\gamma} \sim 0 \qquad \dot{\gamma} = \text{const.} = \omega_\gamma. \tag{5.7}$$

The solution is given by

$$\left.\begin{aligned} \rho_0^2 &= \frac{I}{M} - 2r_0^2 \\ r(t) &= \frac{\epsilon\cdot\lambda\cdot l}{\epsilon(48\kappa-1) - Mb^2\omega_\gamma^2} + \rho_0\cdot\cos(\omega_r t+\alpha); \quad \omega_r^2 = \frac{\epsilon(48\kappa-1)}{Mb^2} - \omega_\gamma^2 \\ \gamma(t) &= \omega_\gamma t + d \\ \phi(t) &= \omega_\gamma t + d + \frac{4M\omega_\gamma\rho_0 r_0}{I\omega_r}\sin(\omega_r t+\alpha) + \frac{M\omega_\gamma\rho_0^2}{I\omega_r}\cdot\sin(\omega_r t+2\alpha) \end{aligned}\right\} \tag{5.8}$$

where α, d are integration constants.

Finally, the qualitative explanation of the short-time behaviour of the ions only lies on the finite dipole and the non-coincidence of the centre of mass and the centre of interaction. It does not take into account:

i) the coupling to the lattice vibrations [53, 58],

ii) the distortion of the lattice [59],

iii) the third dimension,

iv) the appropriate form of the interionic potential.

Thus the model cannot provide quantitative results, e.g. rotational barrier heights [53, 57]. But *it shows the main features without fitting of parameters* [53]. In addition the correction of the *isotopic shift of* ω_{libr} by this model agrees well with the experiment [52].

5.3. *Influence of strong crystalline fields and low temperatures on correlation and memory functions*

The relatively high ω_{libr} and the detailed balance principle (equations (3.8)) cause a considerable asymmetry of the infrared-absorption band. Therefore we actually measure $C_{u,s}(t)$ instead of $\Phi_u(t)$. The quantum corrections of Section 2.5 yield:

$$\left.\begin{aligned} &\text{for } OD^-\text{:} \quad M_2'/M_2 = 1 + 9.27T^{-1} + 1.16T^{-1}\frac{\langle\vec{N}^2\rangle}{(kT)^2} \\ &\text{for } OH^-\text{:} \quad M_2'/M_2 = 1 + 17.7T^{-1} + 2.22T^{-1}\frac{\langle\vec{N}^2\rangle}{(kT)^2} \end{aligned}\right\} \tag{5.9}$$

Those of the high moments diminish with increasing order. The additional terms in the above equations depend on the temperature and the mean square torques. Even for $\langle\vec{N}^2\rangle \gg (kT)^2$ there are temperatures where $M_2' \cong M_2$. On the other hand large torques allow the memory function $K_u(t)$ to approach the angular momentum correlation function $\Phi_J(t)$ if

$$\langle\vec{N}^2\rangle \gg 4(kT)^2. \tag{2.42}$$

Hence there may exist a temperature range where $M_2 \cong M_2'$ and $K_u(t) \cong \Phi_J(t)$.

5.4. *Experimental angular correlation functions and second moments*

Figures 5.2–5.6 show the *experimentally determined correlation functions* of OD^- in various alkalihalides for temperatures between 15°K and 600°K. The relevant data on OH^- and OD^- and the alkalihalides are listed in Tables 5.1 and 5.2. Earlier room-temperature measurements on OH^- and OD^- in KCl have revealed oscillating correlation functions displaying an isotopic shift proportional to $\sqrt{I}$ [60]. This structure

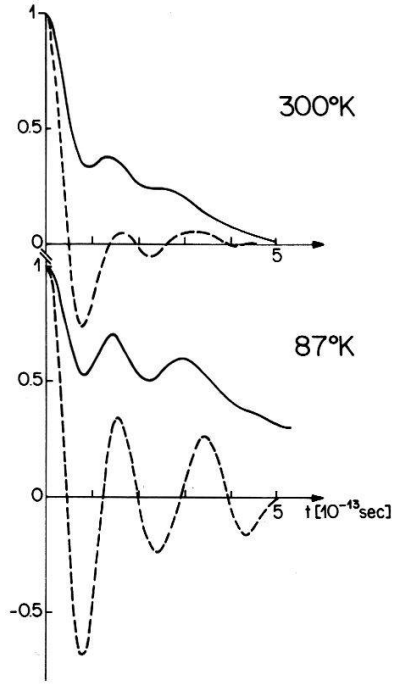

Figure 5.2
Angular autocorrelation functions $C_{u,s}(t)$ (——) and approximate angular momentum correlation functions $\Phi_J(t)$ (-----) of OD^- in RbCl.

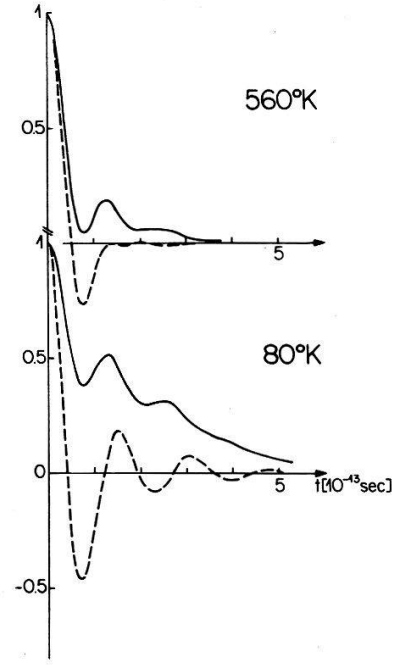

Figure 5.3
Angular autocorrelation functions $C_{u,s}(t)$ (——) and approximate angular momentum correlation functions $\Phi_J(t)$ (-----) of OD^- in KCl.

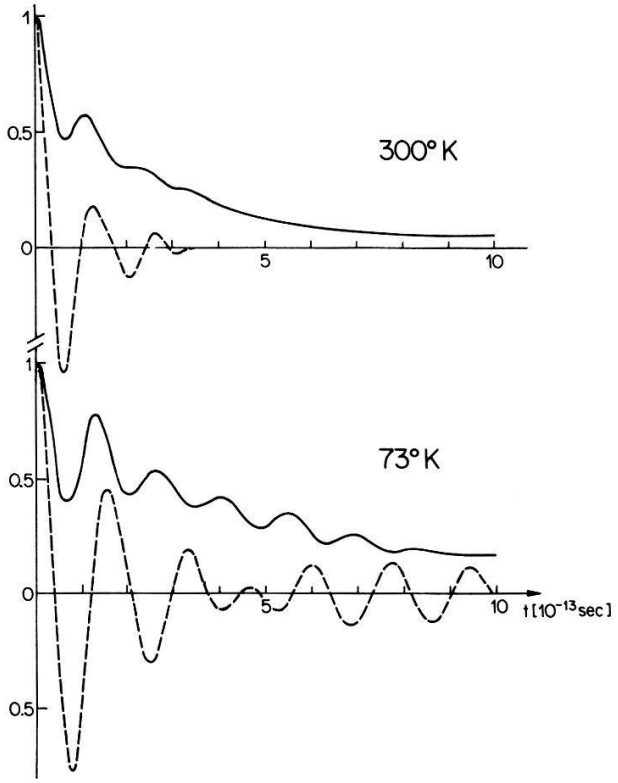

Figure 5.4
Angular autocorrelation functions $C_{u,s}(t)$ (——) and approximate angular momentum correlation functions $\Phi_J(t)$ (-----) of OD^- in KBr.

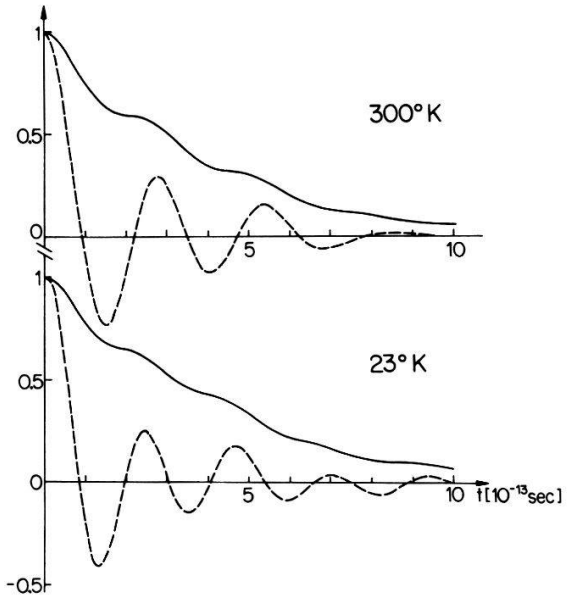

Figure 5.5
Angular autocorrelation functions $C_{u,s}(t)$ (——) and approximate angular momentum correlation functions $\Phi_J(t)$ (-----) of OD^- in NaBr.

characterizes a two-dimensional librator. Potential barriers responsible for the libration have been estimated by several authors [53, 57, 61]. Our experimental correlation functions provide a test of these calculations.

At low temperature all correlation functions oscillate indicating a librational motion. With increasing temperature the oscillations, as well as the complete correlation

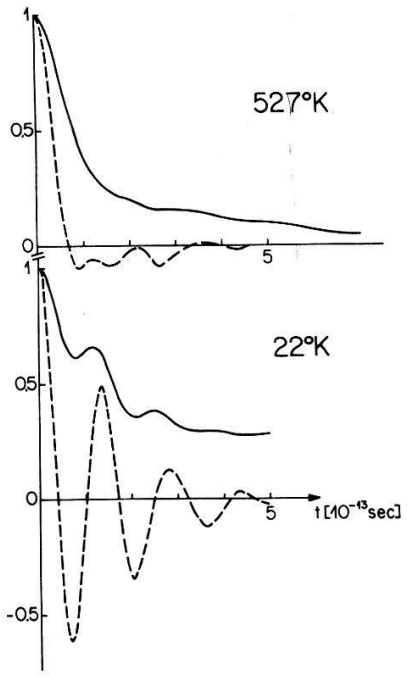

Figure 5.6
Angular autocorrelation functions $C_{u,s}(t)$ (——) and approximate angular momentum correlation functions $\Phi_J(t)$ (-----) of OD^- in KJ.

functions, are progressively damped. In most crystals the oscillations are maintained even at high temperatures whereas for OD^- in KJ they collapse near 530°K. OD^- in KJ has a height of the rotational barrier corresponding to 534°K ([53], Table 5.2). Above 534°K the libration turns into an overall rotation. From the point of view of our

Table 5.1
Properties of OH^- and OD^- ions.

	Moment of inertia, I [10^{-40} cgs]	Rotation constant [cm^{-1}]	Bond length [Å]
OH^-	1.53	18.9	
OD^-	2.91	10.0	0.974

Table 5.2
Properties of the alkalihalide lattices.

	Lattice constant [Å]	Minimum cavity, ϕ [Å]	Rotational barrier [53] [°K]
RbCl	6.54	3.58	911
KCl	6.28	3.62	840
NaCl	5.63	3.73	1068
RbBr	6.85	3.89	
KBr	6.59	3.93	676
NaBr	5.96	4.06	184
RbJ	7.33	4.37	
KJ	7.05	4.39	534
NaJ	6.46	4.56	

model this change corresponds to a transition from the low temperature to the high temperature solution (equations (5.5) and (5.8)).

For a more quantitative analysis we also determined *the second spectral moments* $M_2'(T)$ as functions of the temperature T (Fig. 5.7). At low temperatures the experimental M_2' surpasses by far the classical $M_2(T)$ due to the strong torques $\langle \vec{N}^2 \rangle$ in agreement with equation (5.9). With increasing temperature the $M_2'(T)$ should approach its classical value $M_2(T)$ from the upper side as observed for KCl and RbCl. However, the $M_2'(T)$ of KJ and NaBr remain approximately constant and cross $M_2(T)$. M_2' of KBr represents an intermediate case.

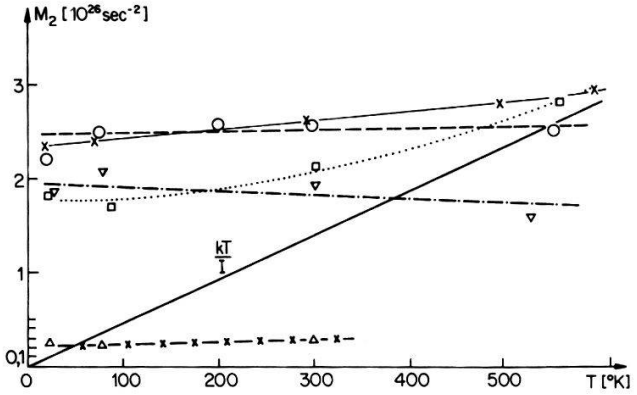

Figure 5.7
The second spectral moment M_2 as a function of the temperature of OD^- in $\cdots$ RbCl, —— KCl, ----- KBr, -×-×-× NaBr, -·-·- KJ, compared to the classical $M_2 = kT/I$ (——).

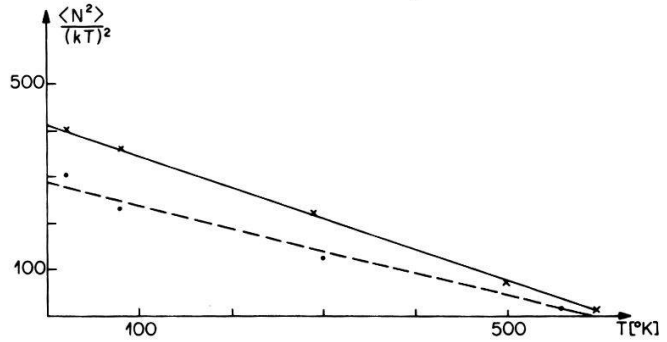

Figure 5.8
Temperature dependence of the mean square torques $\langle N^2 \rangle / (kT)^2$ of OD^- in KCl (——) and RbCl (-----).

The only possible interpretation of this striking feature is to assume *a temperature-dependent increase of the moment of inertia* I in equation (2.49) according to

$$I(T) = I_0 + ma^2(T) \tag{5.10}$$

where $a(T)$ indicates *the distance between the centre of mass and the centre of rotation or libration*. The large cavities allow the increase of $a(T)$ with temperature. Unfortunately this temperature dependence impedes the determination of $\langle \vec{N}^2 \rangle(T)$ from $M_2'(T)$ as suggested by equation (2.49).

On the other hand, if the $M_2'(T)$ of OD^- in KCl and RbCl points to a moment of inertia I independent of the temperature T a *libration about the centre of mass* ensues. This seems also plausible from the tightness of the cavities of KCl and RbCl. Therefore $\langle N^2 \rangle(T)$ can be determined. According to Figure 5.8 $\langle \vec{N}^2 \rangle(T)/(kT)^2$ appears to be a

linear function of T over a wide range. Thus we obtain

$$\langle \vec{N}^2 \rangle(T) = AT^2 - BT^3 \tag{5.11}$$

with

$$A = 778 \cdot 10^{-32} \text{ cgs}, \quad B = 1.27 \cdot 10^{-32} \text{ cgs for KCl}$$

and

$$A = 551 \cdot 10^{-32} \text{ cgs}, \quad B = 0.93 \cdot 10^{-32} \text{ cgs for RbCl}$$

with

$$T_{\max} = 408°\text{K} \quad \text{and} \quad (\langle \vec{N}^2 \rangle)^{1/2}_{\max} = 6.5 \cdot 10^{-13} \text{ cgs for KCl}$$

$$395°\text{K} \qquad\qquad 5.4 \cdot 10^{-13} \text{ cgs for RbCl.}$$

Since $\vec{N}$ represents the gradient of the potential with respect to the angular variation, we may obtain information on the form of the potential well from equation (5.11). In agreement with the librational frequences (Table 5.2) the value of $(\langle \vec{N}^2 \rangle_{\max})^{1/2}$ for RbCl is smaller than for KCl.

5.5. *Memory and angular momentum correlation functions*

Memory functions have two aspects:

the interpretation on the basis of equation (2.26);

interpretation as approximate angular correlation functions $\Phi_J(t)$.

The memory functions in Figures 5.2–5.6 suggest an approximation of the form $K_u(t) = e^{-\alpha t} \cos \omega t$ with the corresponding $\Phi_u(t)$ in Table 2.1 for low and intermediate temperatures. ω is in good agreement with ω_{libr} although the envelopes of $K'_u(t)$ slightly differ from exponentials.

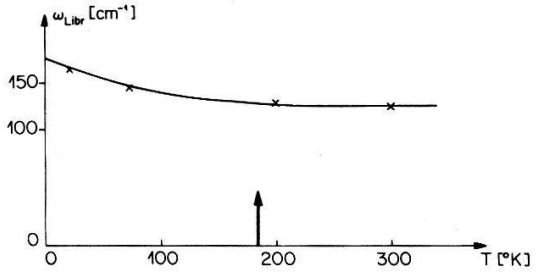

Figure 5.9
Temperature dependence of the librational frequency ω_{libr} of OD^- in NaBr. The arrow indicates the value of the rotational barrier.

The appealing point of $K_u(t)$ is *its interpretation as* $\Phi_J(t)$. The relevant condition (2.42) is well satisfied. The oscillation of $\Phi_J(t) \simeq K'_u(t)$ reflects the motion of the angular momentum of the two-dimensional librator. This fact can be used to determine the librational frequency from $K'_u(t)$ even at temperatures where the separation of the librational side-band from the main vibrational absorption line is no more possible. The ω_{libr} slightly decreases with temperature as illustrated in Fig. 5.9. The hitherto

unknown ω_{libr} of OD^- in NaBr can be determined from the period of $K'_u(t)$ as

$$\omega_{\text{libr}}(OD^-/NaBr) = 160 \pm 5 \text{ cm}^{-1}$$

and the rotational barrier with the aid of Pandy's equation [53] as

$$K = \omega^2_{\text{libr}}/20B = 128 \text{ cm}^{-1} \text{ or } 185°\text{K}.$$

This agrees well with the behaviour of $M'_2(T)$ shown in Figure 5.7.

5.6. *Concluding remarks*

The measurements and the model suggest the occurrence of *three types of motions*:

i) libration about an off-centre centre of mass as in KCl and RbCl at lower temperatures;

ii) libration about a point different from the centre of mass with a temperature-dependent separation $a(\tau)$ as in NaBr, KBr and KJ at intermediate temperatures;

iii) overall rotation about the lattice point with off-centre centre of mass (KJ).

Types i) and iii) are predicted by the two solutions of our model. The motion of type ii) lies outside the scope of the model. It requires the consideration of the higher terms of the potential, i.e. rotational barrier. Nevertheless this does not touch the consistency of the model. The motion of type i) disagrees with the calculations by Pandy [53] since they are based on the *a priori* assumption of separated centres of rotation and mass and our interpretation represents an extrapolation from high temperatures. For a final conclusion further investigations from both sides are necessary.

6. Correlation Functions of Polyatomic Molecules

6.1. *Introduction*

In a first approximation the rotating molecule in a liquid or in a solid can be considered as a rigid top. For an isotropic neighbourhood of the molecule the angular correlation functions related to the random rotation of the molecule can be represented [63] by

$$\Phi_{ij}(t) = \langle \{ R_{ij}(\omega(t)) \} \rangle \tag{6.1}$$

where $R_{ij}(\omega)$ indicates the orthogonal matrix of the orientation $\omega(t)$, which is expressed by a set of rotational parameters, e.g. the Eulerian angles α, β, γ.

The goal of this chapter is to understand the angular correlation functions of polyatomic molecules on the basis of this equation. For this purpose the potential acting on the molecule in the liquid or the solid is assumed not to influence its vibrational and electronic states. Upon the introduction of the appropriate orientational probability densities the consequences of the symmetry of the molecule are found by group theory. The structure of the correlation function matrix $\Phi_{ij}(t)$ suggests the *construction of a number of informative functions* of the rotational parameters and *of a relaxation ellipsoid* [63]. Explicit formulae and experimental results from infrared spectra of simple molecules are presented.

6.2. *Probability densities*

The orientational motion of a molecule is considered as a random process with the random variables α, β, γ and the continuous parameter t. This process is described by a *hierarchy of probability densities* [7, 9, 64]: $w_i(\Omega_1, t_1, \Omega_2, t_2, \ldots, \Omega_1, t_i)$. The two lowest members are:

$w_1(\Omega, t)\, d\Omega$: the probability of finding the molecule at time t with the orientation in the range within Ω and $\Omega + d\Omega$.

$w_2(\Omega_1, t_1/\Omega_2, t_2)\, d\Omega_1\, d\Omega_2$ the probability of finding the molecule at time t_1 with the orientation within the range Ω_1 and $\Omega_1 + d\Omega_1$ and at time t_2 with the orientation within the range Ω_2 and $\Omega_2 + d\Omega_2$.

For *stationary random processes* w_1 is independent of t and w_2 is a function of $\tau = t_2 - t_1$ only. In addition w_2 is symmetric with respect to Ω_1 and Ω_2,

$$w_2(\Omega_1, \tau, \Omega_2) = w_2^*(\Omega_2, \tau, \Omega_1), \tag{6.2}$$

and with respect to the time τ:

$$w_2(\Omega_1, -\tau, \Omega_2) = w_2^*(\Omega_1, +\tau, \Omega_2). \tag{6.3}$$

As probability densities the w_i are *normalized* over the Ω_k:

$$\int w_1(\Omega)\, d\Omega = 1, \quad \int w_2(\Omega_1, \tau, \Omega_2)\, d\Omega_1\, d\Omega_2 = 1 \tag{6.4}$$

and w_2 satisfies:

$$\left.\begin{aligned} \int w_2(\Omega_1, \tau, \Omega_2)\, d\Omega_1 &= w_1(\Omega_2) \\ \int w_2(\Omega_1, \tau, \Omega_2)\, d\Omega_2 &= w_1(\Omega_1). \end{aligned}\right\} \tag{6.5}$$

The w_1 and w_2 are related by the *conditional probability*

$$w_2(\Omega_1, \tau, \Omega_2) = w_1(\Omega_1)\, \bar{w}_2(\Omega_1//\tau, \Omega_2). \tag{6.6}$$

The probability densities of the orientational motion are square integrable functions of the Ω and can therefore be represented with the *Wigner or generalized spherical functions*:

$$D^j_{mm'}(\Omega) = \left[\frac{8\pi^2}{2j+1}\right]^{1/2} D^j_{mm'}(\Omega)_{\text{Wigner}} \quad [65] \tag{6.7}$$

with the *orthogonality reaction*

$$\int D^j_{mm'}(\Omega)^*\, D^{j'}_{nn'}(\Omega)\, d\Omega = \delta_{jj'}\, \delta_{mn}\, \delta_{m'n'} \tag{6.8}$$

and

$$\left.\begin{aligned} w_1(\Omega) &= D^j_{mm'}(\Omega)^*\, w^j_{mm'} \\ w_2(\Omega_1, \tau, \Omega_2) &= D^j_{mm'}(\Omega_1)^*\, w^{jj'}_{mm',nn'}(\tau)\, D^{j'}_{nn'}(\Omega_2) \\ \bar{w}_2(\Omega_1//\tau, \Omega_2) &= D^j_{mm'}(\Omega_1)^*\, \bar{w}^{jj'}_{mm',nn'}(\tau)\, D^{j'}_{nn'}(\Omega_2). \end{aligned}\right\} \tag{6.9}$$

The *average of a function* $f(\Omega)$ is defined as

$$\langle f(\Omega)\rangle = \int f(\Omega)\, w_1(\Omega)\, d\Omega \tag{6.10}$$

and the *correlation function* as

$$\langle f_1(\Omega_1) f_2(\Omega_2)^*\rangle = \iint f_1(\Omega_1)\, W_2(\Omega_1, \tau, \Omega_2)\, f_2(\Omega_2)^*\, d\Omega_1\, d\Omega_2. \tag{6.11}$$

Hence we obtain

$$\left.\begin{aligned} w^j_{mm'} &= \langle D^{j'}_{mm'}(\Omega)\rangle \\ w^{jj'}_{mm',nn'}(\tau) &= \langle D^j_{mm'}(\Omega_1)\, D^{j'}_{nn'}(\Omega_2)^*\rangle. \end{aligned}\right\} \tag{6.12}$$

For an *isotropic surrounding* of the molecule w_1 is constant:

$$w_1 = 1/8\pi^2 \tag{6.13}$$

and w_2 can be expressed by ω,

$$w_2(\Omega_1, \tau, \Omega_2) = w'_2(\omega, \tau) = D^j_{mm'}(\omega)^*\, w'^j_{mm'}(\tau) \tag{6.14}$$

where ω is defined by

$$D^j(\Omega_2) = D^j(\omega)\, D^j(\Omega_1). \tag{6.15}$$

If the molecule possesses a *symmetry group* M then $w'_2(\omega, \tau)$ has to be invariant under all operations $O_M \in M$ represented by the transformation matrices $D^j(O_M)$:

$$D^j(O_M) = \bigoplus_{i(j)} \Gamma_{i(O_M)} \tag{6.16}$$

with $\Gamma_i(O_M)$ = irreducible representation of M contained in D^j according to the rotation group combatibility tables [66].

Schur's lemma provides the invariant $w'^j_{mm'}(\tau)_i$.

For high symmetries and $j = 1$ we obtain

$$\text{cubic molecule: } w^1(t) = \langle 1/3[D^1_{11}(\omega(t)) + D^1_{22}(\omega(t)) + D^1_{33}(\omega(t))]\rangle \tag{6.17}$$

$$\text{axial molecule: } w^1_1(t) = \langle 1/2[D^1_{11}(\omega(t)) + D^1_{22}(\omega(t))]\rangle$$

$$w'^1_3(t) = \langle D^1_{33}(\omega(t))\rangle$$

$$\text{orthorhombic: } w'^1_1(t) = \langle D^1_{11}(\omega(t))\rangle$$

$$w'^1_2(t) = \langle D^1_{22}(\omega(t))\rangle$$

$$w'^1_3(t) = \langle D^1_{33}(\omega(t))\rangle.$$

6.3. *Dipole correlation functions*

The transition dipoles $\vec{\mu}_{if}$ transform as real polar vectors and they belong to irreducible representations of M [67]. For their description the complex $D^1(\omega)$ must be replaced by the real orthogonal matrices $R(\omega)$ related by the similarity transformation

$$R(\omega) = A\, D^1(\omega)\, A^{-1}. \tag{6.18}$$

Each irreducible representation of M present in $R(\omega)$ has a corresponding correlation function which can be measured with a vibrational transition of the same representation [67, 63].

These correlation functions match the coefficients of the conditional probability density $\bar{w}_2(O//\tau,\omega)$. Table 6.1 presents the explicit expressions for this correlation functions in the following parametrizations of the rotation:

α, β, γ	Eulerian angles [68],
ψ, θ, ϕ	rotation angle ψ and polar angles θ and ϕ of the rotation axis [70, 69],
$\psi, \alpha_1, \alpha_2, \alpha_3$	rotation angle ψ and the direction cosines: $\cos\alpha_1$, $\cos\alpha_2$, $\cos\alpha_3$ of the rotation axes [71].

The forms of the $\langle R_{ii}(\omega)\rangle$ for different parametrizations suggest for high symmetries some *informative linear combinations* which are summarized in Table 6.1.

Table 6.1
Explicit forms of the diagonal matrix elements, correlation functions and linear combinations for cubic, axial and orthorhombic molecules.

Matrix elements			
R_{11}	$\cos\gamma\cos\alpha - \cos\beta\sin\alpha\sin\gamma$	$\cos\psi + \sin^2\theta\cos^2\phi(1-\cos\psi)$	$\cos\psi + \cos^2\alpha_1(1-\cos\psi)$
R_{22}	$-\sin\gamma\sin\alpha + \cos\beta\cos\alpha\cos\gamma$	$\cos\psi + \sin^2\theta\sin^2\phi(1-\cos\psi)$	$\cos\psi + \cos^2\alpha_2(1-\cos\psi)$
R_{33}	$\cos\beta$	$\cos\psi + \cos^2\theta(1-\cos\psi)$	$\cos\psi + \cos^2\alpha_3(1-\cos\psi)$

Correlation functions			
Symmetry	cubic	axial	orthorhombic
Representation$_{(\text{dimension})}$	$T_{(3)}$	$A_{(1)}$ $E_{(2)}$	$A_{1(1)}$ $B_{1(1)}$ $B_{2(1)}$
	$\Phi_T(t) = \langle\frac{1}{3}(R_{11}+R_{22}+R_{33})\rangle$	$\Phi_E(t) = \langle\frac{1}{2}(R_{11}+R_{22})\rangle$ $\Phi_A(t) = \langle R_{33}\rangle$	$\Phi_{B_2}(t) = \langle R_{11}\rangle$ $\Phi_{B_1}(t) = \langle R_{22}\rangle$ $\Phi_{A_1}(t) = \langle R_{33}\rangle$
$\langle\cos\psi(r)\rangle$	$\frac{1}{2}(3\Phi_T(t)-1)$	$\frac{1}{2}(\Phi_A(t)+2\Phi_E(t)-1)$	$\frac{1}{2}(\Phi_{A_1}(t)+\Phi_{B_1}(t)+\Phi_{B_2}(t)-1)$
$\langle\sin^2\theta(t)\,(1-\cos\psi(t))\rangle$	$1-\Phi_T(t)$	$1-\Phi_A(t)$	$1-\Phi_{A_1}(t)$
$\langle\cos^2\theta(t)(1-\cos\psi(t))\rangle$	$\frac{1}{2}(1-\Phi_T(t))$	$\frac{1}{2}(1+\Phi_A(t)-2\Phi_E(t))$	$\frac{1}{2}(1+\Phi_{A_1}(t)-\Phi_{B_1}(t)-\Phi_{B_2}(t))$

Finally, the above interpretation of correlation functions outlined in Table 6.1 provides a tool for *comparing molecules of different size and symmetry*. Since differing moments of inertia cause incompatible time-scales, the introduction of an approximate time-scale normalized to a *rotational eigentime* t_0 facilitates the comparison. t_0 is defined as the reciprocal of the mean rotation frequency $\bar{\omega}$:

$$\left.\begin{aligned} t_0^2 &= \frac{12\pi ckT}{\hbar}\tfrac{1}{3}(A+B+C) \quad \text{for non-linear molecules} \\ t_0^2 &= \frac{8\pi ckT}{\hbar}B \qquad\qquad\qquad\quad \text{for diatomic molecules} \end{aligned}\right\} \tag{6.19}$$

where A, B, C are the rotational constants [72] in cm^{-1}.

6.4. *The relaxation ellipsoid*

The introduction of

$$\left.\begin{aligned} \langle \cos \theta_{ij}(\tau) \rangle &= \Phi_{ij}(\tau) \\ \langle \cos^2 (\theta_{ij}(\tau)/2) \rangle &= \tfrac{1}{2}(1 + \Phi_{ij}(\tau)) \\ &= \mathrm{rms}^2[\cos (\theta_{ij}(\tau)/2)] \end{aligned}\right\} \tag{6.20}$$

and the *molecule fixed vectors*

$$\vec{U} = \vec{u} / \mathrm{rms}\{\cos (\theta_{ij}(\tau)/2)\} \tag{6.21}$$

with $\vec{u}$ as an arbitrary unit vector in the molecular coordinate system allows the construction of a *relaxation ellipsoid* [63]:

$$1 = U_i \tfrac{1}{2}(1 + \Phi_{ij}(\tau))\, U_j. \tag{6.22}$$

This ellipsoid describes the time-development of the rotational diffusion tensor in the molecule-fixed system and represents spheres for $t = 0$ and $t = \infty$ with the radii $r = 1$ and $r = \sqrt{2}$ respectively.

6.5. *Experimental results*

The restrictions of Section 3.2 limit the number of suitable molecules. Even the most appropriate molecules of the type CH_x–halogen$_{4-x}$ are partially ruled out because of the natural halogen isotopes and overlapping vibrational bands. The investigation of the correlation functions was restricted to those of the following molecules measured in *pure liquids*:

$$CH_4: \tilde{\nu}_T = 1360\ \mathrm{cm}^{-1}$$

$$CH_3J: \tilde{\nu}_A = 522\ \mathrm{cm}^{-1}, \quad \tilde{\nu}_E = 884\ \mathrm{cm}^{-1},$$

$$CHBr_3: \tilde{\nu}_A = 3023\ \mathrm{cm}^{-1}, \quad \tilde{\nu}_E = 1142\ \mathrm{cm}^{-1},$$

$$CH_2Cl_2: \tilde{\nu}_{A_1} = 283\ \mathrm{cm}^{-1}, \quad \tilde{\nu}_{B_1} = 895\ \mathrm{cm}^{-1}, \quad \tilde{\nu}_{B_2} = 1265.5\ \mathrm{cm}^{-1}.$$

The data for CH_2Cl_2 are taken from Rothschild [25] and the measurements on CH_3J agree well with the data of Faveluke [73].

The functions listed in Table 6.1 were determined from the experimental correlation functions and the results are presented in Figures 6.1 to 6.3. For comparison all $\langle \cos \psi(t) \rangle$ were collected and plotted on the normalized time-scale of equation (6.19) in Figure 6.1. The effects of inertia are ruled out by the normalized time-scale. The relaxation of the rotation angle ψ is most rapid in CH_3J and slowest in CH_2Cl_2 and $CHBr_3$. Because of the large van der Waals radius of the iodine, the structure of the prolate CH_3J is relatively compact thus allowing a fast relaxation about the symmetry axis. In contrast, the shapes of CH_2Cl_2 (Fig. 6.4) and $CHBr_3$ gives rise to considerable steric hindrance which is confirmed by the $\langle \cos \psi(t) \rangle$.

A more detailed picture for the symmetric tops is provided by the functions $\langle \sin^2 \theta(t)(1 - \cos \psi(t)) \rangle$ and $\langle \cos^2 \theta(t)(1 - \cos \psi(t)) \rangle$ in Figure 6.2. For CH_3J the average

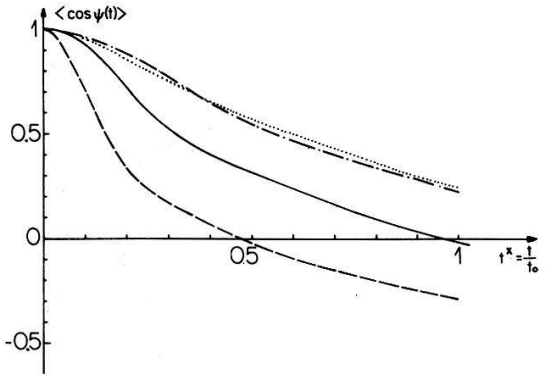

Figure 6.1
Angular autocorrelation functions of the mean rotation angle $\langle \cos \psi(t) \rangle$ of —— CH_4, ----- CH_3J, -.-.- $CHBr_3$, ···· CH_2Cl_2.

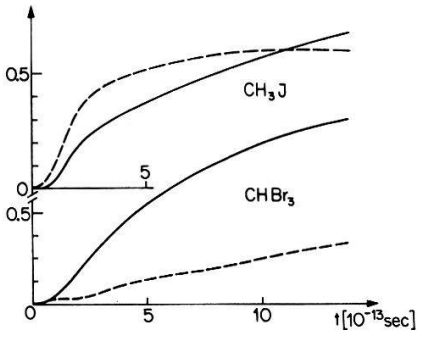

Figure 6.2
The correlation functions $\langle \sin^2\theta(t)\ (1 - \cos \psi(t)) \rangle$ (——) and $\langle \cos^2\theta(t)\ (1 - \cos \psi(t)) \rangle$ (-----) of CH_3J and $CHBr_3$.

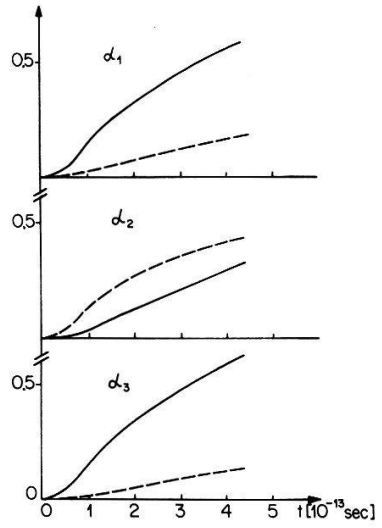

Figure 6.3
The correlation functions $\langle \sin^2 \alpha_i(t)\ (1 - \cos \psi(t)) \rangle$ (——) and $\langle \cos^2 \alpha_i(t)\ (1 - \cos \psi(t)) \rangle$ (-----) of CH_2Cl_2 with respect to its three inequivalent axis X_i.

rotation axis (different from the axis of instantaneous rotation) remains relatively near to the symmetry axis for times up to $8 \cdot 10^{-12}$ s, which is surmised by

$$\langle \cos^2 \theta(t) \, (1 - \cos \psi(t)) \rangle \gg \langle \sin^2 \theta(t) \, (1 - \cos \psi(t)) \rangle .$$

However, for the oblate $CHBr_3$, the average rotation axis moves in a plane perpendicular to the symmetry axis.

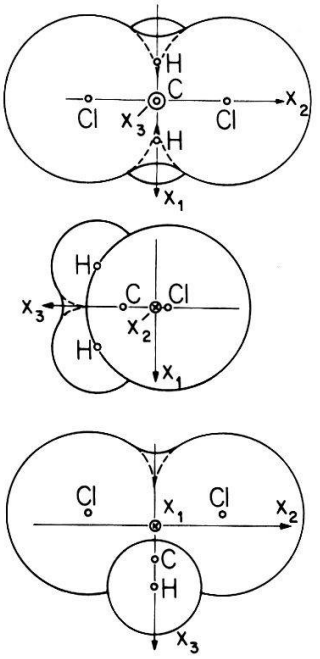

Figure 6.4
Shape of the CH_2Cl_2 molecule as seen in the direction of its three axes X_i.

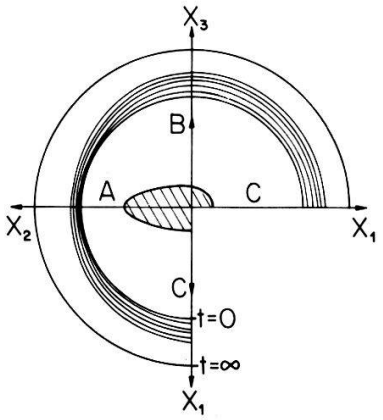

Figure 6.5
Relaxation ellipsoid of CH_2Cl_2. The time step between subsequent curves is $0.2 \cdot 10^{-12}$ s. The moment of inertia ellipsoid is presented in the centre of the figure. A, B and C indicate the rotation constants with the relation $A > B > C$.

For CH_2Cl_2 the curves of Figure 6.3 yield the relations

$$\langle \cos^2 \alpha_1(t) \, (1 - \cos \psi(t)) \rangle < \langle \sin^2 \alpha_1(t) \, (1 - \cos \psi(t)) \rangle$$

$$\langle \cos^2 \alpha_2(t) \, (1 - \cos \psi(t)) \rangle > \langle \sin^2 \alpha_2(t) \, (1 - \cos \psi(t)) \rangle$$

$$\langle \cos^2 \alpha_3(t) \, (1 - \cos \psi(t)) \rangle < \langle \sin^2 \alpha_3(t) \, (1 - \cos \psi(t)) \rangle$$

and therefore suggest a stay of the average rotation axes near the direction of the largest diameter parallel to the Cl–Cl axes. This behaviour is confirmed by the relaxation ellipsoid shown in Figure 6.5. In general the preferred direction of the average rotation axis is close to the axis corresponding to the smallest moment of inertia whereas the relaxation rate is reigned by the steric hindrance.

The correlation functions of the polyatomic molecules indicate that *they rapidly approach a diffusion-like motion* with an exponential decay of the $\Phi_{ij}(t)$, although they perform angular jumps considerably larger than generally assumed in diffusion-type relaxation theories [74–79].

7. Appendix: Correlation functions of Vibrational Raman Spectra

According to Gordon [14] the differential Raman scattering cross-section is related to the correlation functions of the *components of the polarizability tensor* $\alpha(t)$:

$$\lambda_s^4 \frac{d^2\sigma}{d\Omega\, d\omega} = \frac{1}{2\pi} \int_{-\infty}^{+\infty} e^{-i\omega t}\, dt \langle (\vec{e}^{\,i} \cdot \alpha(O) \cdot \vec{e}^{\,s})\, (\vec{e}^{\,i} \cdot \alpha(t) \cdot \vec{e}^{\,s}) \rangle \tag{7.1}$$

The directions of the incident light $\vec{e}^{\,i}$ and of the scattered light $\vec{e}^{\,s}$ determine the component of $\alpha(t)$ measured. Hence a complete group-theoretical set of correlation functions $\langle \alpha_{is}\,(O)\, \alpha_{is}\,(t) \rangle$ describes rotation of α and thus of the molecule.

As a three-dimensional symmetric cartesian tensor of second rank $\alpha(t)$ possesses six components, which can be split in a rotational invariant tensor of rank zero [80],

$$\alpha_0 = \tfrac{1}{3} \operatorname{trace} \alpha(t) \tag{7.2}$$

and the five components of an irreducible three-dimensional tensor of rank 2

$$\left.\begin{aligned} A_1 &= \tfrac{1}{2}(3\alpha_{zz}(t) - 1) & A_3 &= \alpha_{xy}(t) \\ A_2 &= \tfrac{1}{2}(\alpha_{xx}(t) - \alpha_{yy}(t)) & A_4 &= \alpha_{xz}(t) \\ & & A_5 &= \alpha_{yz}(t). \end{aligned}\right\} \tag{7.3}$$

The *isotropic part* $\alpha_0(t)$ gives rise to the *polarized* and the *anisotropic part* $\{A_i\}$ to the *depolarized Raman scattering intensity*. The tensor components A_i transform as

$$A_i = R_{ik}^{j=2}(\omega)\, E_k \tag{7.4}$$

where the E_k represent a space-fixed tensorial basis and the $R^{j=2}(\omega)$ the real orthogonal matrix of dimension 5. Naturally $R^{j=2}(\omega)$ is related to the $D^2(\omega)$ by a similarity transformation analogous to that of equation (6.18). Therefore the relationship of $R^{j=2}(\omega(t))$ to the $w_i'^2(t)$ (6.14) is determined by the irreducible representations Γ_i contained in $R^{j=2}(\omega)$ (6.16). The explicit expressions for the diagonal elements of $R^{j=2}(\omega)$ are presented in Table 7.1

As an *example* we consider a molecule of cubic symmetry. The Raman lines of the species E provide a correlation function

$$\Phi_E(t) = \tfrac{1}{2}\langle R_{11}^2(t) + R_{22}^2(t) \rangle$$

Table 7.1
Explicit forms of the diagonal matrix elements for $l = 2$, as measured by vibrational Raman spectra.

	Diagonal elements of $R^2(\psi, \theta, \phi)$	
R^2_{11}	$\frac{1}{2}(3(R^1_{33})^2 - 1)$	$\frac{1}{2}[3\cos^2\psi + 6\cos^2\theta\cos\psi(1-\cos\psi) + 3\cos^4\theta(1-\cos\psi)^2 - 1]$
R^2_{22}	$\frac{1}{2}((R^1_{11})^2 + (R^1_{22})^2 - (R^1_{12})^2 - (R_{21})^2)$	$\frac{1}{2}[2\cos^2\psi + 2\sin^2\theta\cos\psi(1-\cos\psi) + \sin^4\theta(1-\cos\psi)^2 - 2\cos^2\theta\sin^2\psi]$
R^2_{33}	$R^1_{11}\cdot R^1_{22} + R^1_{12}R^1_{21}$	$\cos^2\psi + 2\sin^2\theta\cos\psi(1-\cos\psi) + 2\sin^4\theta\sin^2\phi\cos^2\phi(1-\cos\psi)^2 - \cos^2\theta\sin^2\psi$
R^2_{44}	$R^1_{11}R^1_{33} + R^1_{13}R^1_{31}$	$\cos^2\psi + [\cos^2\theta + \sin^2\theta\cos^2\phi]\cos\psi(1-\cos\psi) + 2\sin^2\theta\cos^2\theta\cos^2\phi(1-\cos\psi)^2 - \sin^2\theta\sin^2\psi\sin^2\phi$
R^2_{55}	$R^1_{22}R^1_{33} + R^1_{23}\cdot R^1_{32}$	$\cos^2\psi + [\cos^2\theta + \sin^2\theta\sin^2\phi]\cos\psi(1-\cos\psi) + 2\sin^2\theta\cos^2\theta\sin^2\phi(1-\cos\psi)^2 - \sin^2\theta\cos^2\phi\sin^2\psi$
	$\sum_i R^2_{ii} = 1 + 2\cos\psi + 2\cos 2\psi$	

and those of the species

$$\Phi_{T_2}(t) = \tfrac{1}{3}\langle R^2_{33}(t) + R^2_{44}(t) + R^2_{55}(t)\rangle.$$

By a linear combination of the two above correlation functions we obtain

$$\langle 1 + 2\cos\psi(t) + 2\cos 2\psi(t)\rangle = 2\Phi_E(t) + 3\Phi_{T_2}(t).$$

Acknowledgments

We are very grateful to Prof. Dr. W. Känzig (Zürich), K. Knop (Zürich), Prof. Dr. L. Galatry (Besancon), Prof. Dr. A. Rahman (Argonne), Dr. M. Hoare (London), Dr. P. Nienhuis (Leiden), Dr. W. G. Rothschild (Dearborn) and Dr. A. G. St. Pierre (Erlangen) for fruitful discussions. We also wish to acknowledge the help of H. Baltes, P. Ebersold, W. Herrmann, R. Hartmann, R. Kälin, Miss M. Leder, K. Müller, Miss O. Rösli, J. Roth, P. Rütimann, B. Rusch, E. Rohr, H. J. Schötzau and P. Stettler.

REFERENCES

[1] P. Debye, *Polar Molecules* (Dover Publ., New York 1954).
[2] R. Zwanzig, Ann. Rev. Phys. Chem. *16*, 67 (1965).
[3] R. Kubo, J. Phys. Soc. Japan *12*, 570 (1957).
[4] R. Kubo, *Lectures in Theoretical Physics*, Vol. I, edited by W. E. Brittin and L. G. Dunham (Interscience, New York 1961), p. 20.
[5] R. Gordon, J. Chem Phys. *43*, 1307 (1965).
[6] H. Shimizu, J. Chem. Phys. *43*, 2453 (1965); Bull. Chem. Soc. Japan *39*, 2385 (1966); J. Chem. Phys. *48*, 2494 (1968).

[7] H. CRAMER and H. LEADBETTER, *Stationary Random Processes* (J. Wiley, New York 1968).
[8] J. L. DOOB, *Stochastic Processes* (J. Wiley, New York 1953).
[9] A. SCHWESCHNIKOW, *Untersuchungsmethoden der Theorie der Zufallsfunktionen* (Akad. Verlagsges, Leipzig 1965).
[10] A. KHINTCHIN, Math. Ann. *109*, 604 (1934).
[11] B. J. BERNE and G. P. HARP, *Advances in Chemical Physics*, Vol. 12 (Interscience, New York 1970), p. 67.
[12] P. MAZUR, Cargese Lectures in Theoretical Physics (Gordon and Breach, New York 1966).
[13] P. C. MARTIN, in *Statistical Mechanics of Equilibrium and Non-Equilibrium*, edited by J. MEIXNER (North Holland, Amsterdam 1965); Les Houches Lectures 1967 (Gordon and Breach, New York 1968).
[14] R. G. GORDON, *Advances in Magnetic Resonance*, Vol. 3, edited by J. S. WAUGH (Academic Press, New York 1968).
[15] L. ONSAGER, Phys. Rev. *37*, 405 (1931).
[16] R. BESSENRODT, Z. Physik *235*, 110 (1970); *238*, 258 (1970).
[17] R. BESSENRODT, Z. Physik *242*, 56 (1971).
[18] G. DOETSCH, *Einführung in Theorie und Anwendung der Laplace-Transformation* (Birkhäuser, Basel 1970).
[19] M. CH. WANG and G. E. UHLENBECK, Rev. Mod. Phys. *17*, 323 (1945).
[20] B. J. BERNE, J. P. BOON and S. A. RICE, J. Chem. Phys. *45*, 1086 (1966).
[21] R. GORDON, J. Chem. Phys. *39*, 2788 (1963); *40*, 1973 (1964); *41*, 1819 (1964).
[22] P. SCHOFIELD, Phys. Rev. Lett. *4*, 39 (1960).
[23] P. A. EGELSTAFF, Advan. Phys. *11*, 203 (1962).
[24] P. NIENHUIS, private communication, 1969.
[25] W. G. ROTHSCHILD, J. Chem Phys. *53*, 990 (1970).
[26] R. J. KRIEGLER and H. L. WELSH, Can. J. Phys. *46*, 1181 (1968).
[27] W. G. ROTHSCHILD, J. Chem. Phys. *49*, 2250 (1968).
[28] B. KELLER and F. KNEUBÜHL, J. Phys. *B3*, 688 (1970).
[29] B. KELLER, P. EBERSOLD, K. MÜLLER and F. KNEUBÜHL, *Proceedings of the Symposium on Submillimeter Waves*, Vol. XX of MRI Symposia (Polytechnic Institute of Brooklyn 1970), p. 437.
[30] M. O. BULANIN, N. D. ORLOVA and D. N. SHCHEPKIN, Optics and Spectroscopy *19*, 406 (1965).
[31] J. LASCOMBE, P. V. HUONG and M. L. JOSIEN, Bull. Soc. Chim. *1959*, 1175.
[32] G. HERZBERG, *Spectra of Diatomic Molecules* (Van Nostrand, New York 1950).
[33] G. HERZBERG, *Infrared and Raman Spectra of Polyatomic Molecules* (Van Nostrand, New York 1945).
[34] A. H. NARTEN, M. D. DANFORD and H. A. LEVY, J. Chem. Phys. *46*, 4875 (1967).
[35] C. T. RUTLEDGE and G. T. CLAYTON, J. Chem. Phys. *52*, 1927 (1970).
[36] J. E. GRIFFITHS and Y. H. PAO, J. Chem. Phys. *46*, 1679 (1967); *49*, 642 (1968).
[37] S. KAPPHAN and F. LÜTHY, Solid State Comm. *8*, 349 (1970); S. KAPPHAN, Thesis University of Utah (1970).
[38] P. HANDLER and D. E. ASPNES, Phys. Rev. Lett. *17*, 1095 (1966).
[39] M. V. KLEIN, B. WEDDING and M. A. LEVINE, Phys. Rev. *180*, 902 (1969).
[40] B. WEDDING, Thesis University of Illinois (1969).
[41] C. K. CHAU, M. V. KLEIN and B. WEDDING, Phys. Rev. Lett. *18*, 521 (1966).
[42] B. WEDDING and M. V. KLEIN, Phys. Rev. *177*, 1274 (1969).
[43] D. R. BOSOMWORTH, Solid State Comm. *5*, 681 (1967).
[44] D. HARRISON and F. LÜTHY, Int. Symp. on Color Centers in Alkalihalides, Rome 1968.
[45] R. D. KIRBY, A. E. HUGHES and A. J. SIEVERS, Report 1314, Cornell University, New York 1970.
[46] R. L. ROSENBAUM, C. K. CHAU and M. V. KLEIN, Phys. Rev. *186*, 852 (1969).
[47] R. S. SCOTT and W. H. FLYGARE, Phys. Rev. *182*, 445 (1969).
[48] G. FEHER, I. W. SHEPHERD and H. B. SHORE, Phys. Rev. Lett. *16*, 500 (1966).
[49] W. E. BRON and R. W. DREYFUS, Phys. Rev. Lett. *16*, 165 (1966).
[50] W. KANZIG, H. R. HART and S. ROBERTS, Phys. Rev. Lett. *13*, 543 (1964).
[51] U. KUHN and F. LÜTY, Solid State Comm. *2*, 281 (1964).
[52] B. KELLER and F. KNEUBÜHL, Solid State Comm. *8*, 867 (1970).
[53] G. K. PANDY and D. K. SHUKLA, Phys. Rev. *B3*, 4391 (1971).
[54] M. ABRAMOWITZ and I. A. STEGUN, *Handbook of Mathematical Functions* (Dover Publ., New York 1965).

[55] F. M. ARSCOTT, *Periodic Differential Equations* (Pergamon Press, London 1964).
[56] K. F. RENK, Z. Physik *201*, 445 (1967).
[57] S. CHANDRA, G. K. PANDEY and V. K. AGRAWAL, J. Phys. Chem. Solids *30*, 1644 (1968).
[58] B. G. DICK, Phys. Stat. Solidi *29*, 587 (1968).
[59] H. B. SHORE, Phys. Rev. Lett. *17*, 1142 (1966).
[60] B. KELLER and F. KNEUBÜHL, Phys. Rev. Lett. *21*, 88 (1968).
[61] P. SAUER, Z. Physik *199*, 256 (1967).
[62] O. F. SCHIRMER, Phys. Lett. *33A*, 439 (1970).
[63] B. KELLER and F. KNEUBÜHL, Chem. Phys. Lett. *9*, 178 (1971).
[64] W. A. STEELE, J. Chem. Phys. *38*, 2404, 2411 (1963).
[65] E. P. WIGNER, *Group Theory* (Academic Press, London 1959).
[66] G. F. KOSTER, J. O. DIMMOCK, R. G. WHEELER and H. STATZ, *Properties of Thirty-two Poin Groups* (M.I.T. Press, Cambridge, Mass. 1963).
[67] E. B. WILSON, J. C. DECIUS and P. C. CROSS, *Molecular Vibrations* (McGraw-Hill, New York 1955).
[68] H. GOLDSTEIN, *Klassische Mechanik* (Akad. Verlagsges, Frankfurt, 1960).
[69] M. CARMELI, J. Math. Phys. *9*, 1987 (1968).
[70] H. E. MOSES, Il Nuovo Cimento *XL A*, 1120 (1965); Ann. Phys. *37*, 224 (1966); Ann. Phys. *42*, 343 (1967).
[71] E. MADELUNG, *Die mathematischen Hilfsmittel des Physikers* (Dover Publ., New York 1943).
[72] C. H. TOWNES and A. L. SCHAWLOW, *Microwave Spectroscopy* (McGraw-Hill, New York 1955).
[73] G. E. FAVELUKES, A. A. CLIFFORD and B. CRAWFORD JR., J. Phys. Chem. *72*, 962 (1966).
[74] W. H. FURRY, Phys. Rev. *107*, 7 (1957).
[75] L. D. FAVRO, Phys. Rev. *119*, 53 (1960).
[76] K. MISHIMA, J. Phys. Soc. Japan *31*, 1796 (1971).
[77] R. E. D. MCCLUNG, J. Chem. Phys. *51*, 3842 (1969).
[78] M. FIXMANN and K. RIDER, J. Chem. Phys. *51*, 2425 (1969).
[79] R. GORDON, J. Chem. Phys. *44*, 1830 (1966).
[80] U. FANO and G. RACAH, *Irreducible Tensorial Sets* (Academic Press, London 1959).
[81] S. BRATOS, Phys. Rev. *A4*, 1078 (1971).
[82] A. LAUBERAU, private communication.
[83] P. VON KONYNENBURG and W. A. STEELE, J. Chem. Phys. *56*, 4776 (1972).